

Journal of Fluid Mechanics

<http://journals.cambridge.org/FLM>

Additional services for *Journal of Fluid Mechanics*:

Email alerts: [Click here](#)

Subscriptions: [Click here](#)

Commercial reprints: [Click here](#)

Terms of use : [Click here](#)



Induced flow due to blowing and suction flow control: an analysis of transpiration

James D. Woodcock, John E. Sader and Ivan Marusic

Journal of Fluid Mechanics / Volume 690 / January 2012, pp 366 - 398

DOI: 10.1017/jfm.2011.441, Published online: 25 November 2011

Link to this article: http://journals.cambridge.org/abstract_S0022112011004411

How to cite this article:

James D. Woodcock, John E. Sader and Ivan Marusic (2012). Induced flow due to blowing and suction flow control: an analysis of transpiration. *Journal of Fluid Mechanics*, 690, pp 366-398
doi:10.1017/jfm.2011.441

Request Permissions : [Click here](#)

Induced flow due to blowing and suction flow control: an analysis of transpiration

James D. Woodcock^{1,2,†}, John E. Sader¹ and Ivan Marusic²

¹ Department of Mathematics and Statistics, University of Melbourne, Melbourne, Vic 3010, Australia

² Department of Mechanical Engineering, University of Melbourne, Melbourne, Vic 3010, Australia

(Received 27 April 2011; revised 16 August 2011; accepted 5 October 2011;
first published online 25 November 2011)

It has previously been demonstrated that the drag experienced by a Poiseuille flow in a channel can be reduced by subjecting the flow to a dynamic regime of blowing and suction at the walls of the channel (also known as ‘transpiration’). Furthermore, it has been found to be possible to induce a ‘bulk flow’, or steady motion through the channel, via transpiration alone. In this work, we derive explicit asymptotic expressions for the induced bulk flow via a perturbation analysis. From this we gain insight into the physical mechanisms at work within the flow. The boundary conditions used are of travelling sine waves at either wall, which may differ in amplitude and phase. Here it is demonstrated that the induced bulk flow results from the effect of convection. We find that the most effective arrangement for inducing a bulk flow is that in which the boundary conditions at either wall are equal in magnitude and opposite in sign. We also show that, for the bulk flow induced to be non-negligible, the wavelength of the boundary condition should be comparable to, or greater than, the height of the channel. Moreover, we derive the optimal frequency of oscillation, for maximising the induced bulk flow, under such boundary conditions. The asymptotic behaviour of the bulk flow is detailed within the conclusion. It is found, under certain caveats, that if the amplitude of the boundary condition is too great, the bulk flow induced will become dependent only upon the speed at which the boundary condition travels along the walls of the channel. We propose the conjecture that for all similar flows, if the magnitude of the transpiration is sufficiently great, the bulk flow will depend only upon the speed of the boundary condition.

Key words: drag reduction, Navier–Stokes equations

1. Introduction

A novel method of active drag reduction has previously been discovered to affect both laminar and turbulent flows (Choi, Moin & Kim 1994). This method, now known as ‘transpiration’, involves subjecting the flow to a non-zero and non-constant wall-normal velocity at the flow’s surface. This boundary condition consists of both blowing and suction at the surface, and imparts no net volume flux upon the flow. This effect has so far been investigated via numerical and analytical methods, and to the authors’ knowledge its existence has thus far not been verified experimentally.

† Email address for correspondence: j.woodcock@student.unimelb.edu.au

It had previously been suspected that transpiration should be incapable of producing a sustainable sublamina drag within a Poiseuille flow (Bewley 2001). (A Poiseuille flow is a flow that is driven by an imposed pressure gradient, and by ‘sublamina’ drag, we mean that the drag is less than would be experienced by a lamina Poiseuille flow in the absence of transpiration.) Indeed, initial attempts to produce simulations of flows with minimised drag resulted in only transient periods of sublamina drag (Cortelezzi *et al.* 1998; Aamo, Krstić & Bewley 2003).

However, more recently Min *et al.* (2006) demonstrated that it is possible, within a lamina Poiseuille flow, for transpiration to produce a sublamina drag that is persistent and sustainable. The boundary conditions they employed were of a travelling sine wave at the top wall of the channel, matched with a sine wave of equal magnitude and opposite sign at the bottom wall, which moved counter to the overall direction of the flow. (This arrangement has been referred to as ‘varicose mode’.) These boundary conditions had been chosen as a result of analysing an expression for the drag acting on the fluid that was developed by Fukagata, Iwamoto & Kasagni (2002), and which related the drag to a weighted integral of the Reynolds stress.

Specifically, Min *et al.* (2006) demonstrated numerically that sustained sublamina drag could be produced within low-Reynolds-number lamina flows, and produced simulations of turbulent flows in which transpiration resulted in significant sustained drag reduction.

Min *et al.* (2006) conclude their paper with the observation that transpiration would be physically difficult to implement. They suggest instead that ‘a moving surface with wavy motion would produce a similar effect, since wavy walls with small amplitudes can be approximated by surface blowing and suction.’ In other words, the effect of transpiration may be approximated by that of peristalsis, provided that the maximum amplitude of the deformation is small. By solving the Navier–Stokes equation through both numerical simulations and a perturbation analysis, Hoepffner & Fukagata (2009) compared such peristalsis-driven flows to those driven by transpiration. They report that despite the apparent similarity between transpiration and peristalsis (they are both driven by a non-zero wall-normal velocity at the walls), their effects are noticeably different. Specifically, they report that the bulk flow induced by peristalsis generally moves in the same direction as the variation in the boundary conditions, while the flow induced by transpiration moves counter to the boundary condition (although the results of their perturbation analysis suggest that it would be possible, under certain conditions, for small-amplitude peristalsis to induce flow in the opposite direction to the variation in the boundary condition). The nature of flows through tubes induced by such rapid oscillations in the tube’s radius have been further studied by Whittaker *et al.* (2010b), and extended to flows through elliptical tubes by Whittaker *et al.* (2010a).

By determining the Reynolds shear stress numerically, Mamori, Fukagata & Hoepffner (2010) investigated the effect of transpiration upon Poiseuille flows in a channel. They considered the combination of a travelling sine wave at one wall in conjunction with an equal and opposite travelling sine wave at the other, which had also previously been used by Min *et al.* (2006). They also considered a system in which a travelling sine wave at one wall is combined with an identical sine wave at the other (an arrangement known as ‘sinuous mode’). They found that the former arrangement produces significantly greater drag reduction than the latter.

Lee, Min & Kim (2008) studied the stability of Poiseuille flows subjected to transpiration. They found that if the boundary conditions consist of upstream-travelling waves, there will be a destabilising effect upon the flow once the amplitude of the boundary condition reaches 1.5% of the centreline velocity. Conversely, if the

boundary conditions consist of downstream-travelling waves, they will have the opposite effect, potentially stabilising an otherwise unstable Poiseuille flow. They found that this stabilising effect was achieved when the phase speed (the speed at which the sine wave boundary condition travels along the wall) exceeded the centreline velocity. They also report that although upstream-travelling wave boundary conditions decrease the drag acting on the fluid, downstream-travelling waves have the opposite effect, resulting in increased drag.

Moarref & Jovanović (2010) also studied the effect of both upstream- and downstream-travelling waves upon Poiseuille flows in a channel. Using a perturbation analysis for boundary conditions of small amplitude, they similarly showed that the drag-reducing upstream-travelling waves potentially destabilise the flow, while the drag-increasing downstream-travelling waves can render stability to otherwise unstable flows. They also derived the rate at which transpiration imparts energy to the flow, and thereby determined the energy efficiency of the resulting drag reduction. The theoretical predictions resulting from their analysis have been verified by a series of direct numerical simulations presented in a companion paper by Lieu, Moarref & Jovanović (2010).

Bewley (2009) proved that the power cost of producing sublaminal drag via transpiration in a Poiseuille flow through a channel for an incompressible Newtonian fluid must necessarily be greater than the power saved due to that drag reduction. This result can be seen as a natural extension of the principle of minimum dissipation (Helmholtz 1868; Batchelor 1967), which states that the velocity field of a Stokes flow will orient itself such that the total rate of dissipation within the flow will be minimised. (While it is true that a laminar Poiseuille flow within a channel will not necessarily be a Stokes flow, since the magnitude of the convective term in such systems is rendered zero by their geometry, they nonetheless obey Stokes equation. They therefore will orient themselves in the same manner as a Stokes flow, and hence the principle of minimum dissipation should be expected to apply.)

Fukagata, Sugiyama & Kasagi (2009) derived the lower bound of the net driving power for a flow through a duct with arbitrary cross-section. They showed that ‘the lowest net power required to drive an incompressible constant mass-flux flow in a periodic duct having arbitrary constant-shape cross-section, when controlled via a distribution of zero-net mass-flux blowing/suction over the no-slip channel walls or via any body forces, is exactly that of the Stokes flow.’

Marusic, Joseph & Mahesh (2007) derived the conditions under which transpiration will produce sublaminal drag. Their formula relates the rate at which the transpiration provides energy to the flow to the rate at which the flow’s energy dissipates. We shall make use of their formula subsequently in § 4.

It is the ability of active forms of drag reduction, such as transpiration, to impart energy upon the flow that enables them to produce sublaminal drag. Numerous passive forms of drag reduction exist, which reduce the drag experienced by a turbulent flow without imparting energy upon the flow. These include adding riblets to the flow’s wall (Karniadakis & Choi 2003), as well the addition of particles such as elastic polymers (Toms 1948; White & Mungal 2008) and surfactant micelles (Warholic, Schmidt & Hanratty 1999) to the fluid, which can reduce the drag via the imposition of a body force within the flow. Woodcock, Sader & Marusic (2010) proved that such passive forms of drag reduction, which act through a body force, are invariably incapable of producing sublaminal drag in the flow of an incompressible Newtonian fluid through a channel or pipe.

Transpiration can also be viewed as an example of a variety of flow phenomena known as ‘acoustic streaming’ (Riley 2001). These consist of a fluid that is subjected to a fluctuating force or boundary condition, which induces a change in the fluid’s overall bulk flow. Despite its misleading name, these phenomena are not limited to flows subjected to acoustic vibrations, and neither are they limited to compressible fluids, but include all flows subjected to oscillating body forces and boundary conditions.

The purpose of this present study is to derive explicit asymptotic formulae for the behaviour of flows induced by transpiration. We consider an overall streamwise flow that is induced by transpiration alone, as was reported by Hoepffner & Fukagata (2009). The boundary conditions employed are those in which the wall-normal velocities are travelling sine waves. The waves defining the velocities at either wall are of equal wavelength and frequency, but may differ in magnitude and phase. This is a generalisation of the boundary conditions employed in their investigations by Min *et al.* (2006) and Hoepffner & Fukagata (2009). Using a perturbation analysis, the asymptotic behaviour of such flows has been derived. The bulk flow induced by transpiration is derived in §3, along with the optimal arrangement, wavelength and frequency of the boundary conditions for maximising the bulk flow. The asymptotic behaviour of the bulk flow is detailed in the conclusion. The energy imparted to the flow is derived in §4.

We also examine, in §5, the behaviour of such flows in which the magnitude of the transpiration is considerably greater than the speed at which the boundary condition moves down the channel. We prove that the bulk flow induced by such boundary conditions depends only upon the speed at which the boundary condition moves down the channel. Our analysis here applies to two-dimensional systems whose boundary conditions are the same as those employed in the aforementioned perturbation analysis, and can only be readily extended to a limited set of functionally similar two-dimensional boundary conditions. These represent only a small subset of all possible periodic functions that could define the transpiration boundary conditions. The extension of this proof to generalized boundary conditions, as well as to three-dimensional flows, is posed as a conjecture.

2. Equations of channel flow

We consider the steady-state flow of an incompressible Newtonian fluid through a channel of infinite length and width and finite height. The flow is driven by the boundary conditions at the base and top of the channel that are non-zero in only the wall-normal or z direction, and vary spatially only in the streamwise or x direction.

We assume that the flow remains two-dimensional and laminar. The spanwise or y direction is therefore not included in our derivation. We consider only boundary conditions in which the wall-normal velocity can be represented as a single sine wave travelling backwards in the x direction.

The Navier–Stokes and continuity equations are given by

$$\rho \left(\frac{\partial}{\partial t} \hat{\mathbf{u}} + \hat{\mathbf{u}} \cdot \hat{\nabla} \hat{\mathbf{u}} \right) = -\hat{\nabla} \hat{p} + \mu \hat{\nabla}^2 \hat{\mathbf{u}}, \quad (2.1)$$

$$\hat{\nabla} \cdot \hat{\mathbf{u}} = 0, \quad (2.2)$$

where ρ and μ represent the density and the dynamic viscosity of the fluid, respectively. These equations will subsequently be non-dimensionalized via the

properties of the boundary conditions. Throughout this work, quantities expressed in terms of dimensional units, such as the velocity $\hat{\mathbf{u}}(\hat{\mathbf{x}}, \hat{t})$ and pressure $\hat{p}(\hat{\mathbf{x}}, \hat{t})$ above, are differentiated from their non-dimensionalized counterparts, $\mathbf{u}(\mathbf{x}, t)$ and $p(\mathbf{x}, t)$, by the presence of a circumflex. The position vector is denoted by $\hat{\mathbf{x}}$, and is defined such that $\hat{\mathbf{x}} = (\hat{x}, \hat{z})$.

The height of the infinitely long channel is h , and hence the domain of the flow is given by

$$-\infty < \hat{x} < \infty, \quad 0 \leq \hat{z} \leq h. \quad (2.3)$$

2.1. Boundary conditions

The no-slip boundary condition applies to the streamwise flow. For the wall-normal velocity, we consider a family of possible boundary conditions, which consist of a single-mode travelling sine wave at either wall. The sine wave at the top wall has an amplitude of A , while its counterpart at the bottom wall has an amplitude of γA . Hence γ is simply a dimensionless ratio of the two amplitudes. The sine waves travel backwards along the wall in the streamwise direction, and are of equal wavelength, λ , and temporal frequency, ω (henceforth referred to simply as the ‘frequency’). They may however differ in phase by some quantity ϕ . The wall-normal velocities at the boundaries are therefore given by

$$\hat{w} = \begin{cases} A \sin\left(\frac{\hat{x}}{\lambda} + \omega\hat{t}\right), & \text{at } \hat{z} = h, \\ \gamma A \sin\left(\frac{\hat{x}}{\lambda} + \omega\hat{t} - \phi\right), & \text{at } \hat{z} = 0. \end{cases} \quad (2.4)$$

The parameters γ and ϕ may take the following values:

$$0 \leq \gamma \leq 1, \quad 0 \leq \phi < 2\pi. \quad (2.5)$$

We analyse and compare the resulting flows from four different arrangements of boundary conditions. The first case, which we shall call the ‘mixed’ boundary condition, involves transpiration only on the top wall of the channel, while the no-slip boundary condition applies to w at the bottom wall. The second involves identical boundary conditions at the top and bottom walls, and is referred to here as the in-phase boundary condition. The third involves a travelling sine wave at the top wall and an equivalent cosine wave at the bottom wall, and is referred to here as the out-of-phase boundary condition. The fourth involves boundary conditions that are equal in magnitude but opposite in sign at either wall, and is referred to here as the antiphase boundary condition. (It was under this arrangement that Min *et al.* (2006) demonstrated sustainable sublaminal drag.) Diagrams of an instantaneous realization of each of these cases can be seen in figure 1, and the values of γ and ϕ corresponding to each case are given in table 1.

2.2. The scaled equations

The system contains two natural length scales: h , the height of the channel, and λ , the wavelength of the sinusoidal waves defining the boundary conditions. The other parameters that have been used to non-dimensionalize the quantities of the Navier–Stokes equation are the maximum amplitude (velocity), A , of the boundary condition, the frequency, ω , of the boundary condition, and the density, ρ , and dynamic viscosity, μ , of the fluid.

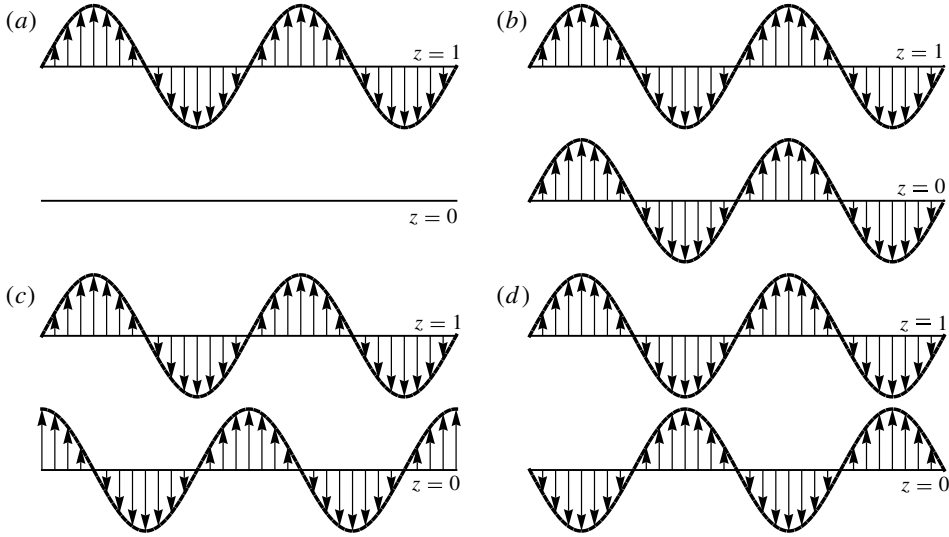


FIGURE 1. Instantaneous realizations of various cases of the family of boundary conditions defined by (2.13): (a) ‘mixed’ boundary conditions; (b) in-phase boundary conditions; (c) out-of-phase boundary conditions; and (d) antiphase boundary conditions.

| Boundary conditions | γ | ϕ |
|---------------------|----------|---------|
| Mixed | 0 | — |
| In-phase | 1 | 0 |
| Out-of-phase | 1 | $\pi/2$ |
| Antiphase | 1 | π |

TABLE 1. Values of γ (the ratio of boundary condition amplitudes) and ϕ (the phase difference) for the four varieties of boundary conditions.

Using these quantities, the variables in the Navier–Stokes equation are scaled according to

$$\hat{x} = hx, \quad \hat{u} = Au, \quad \hat{p} = \frac{\mu A}{h} p, \quad \hat{t} = \frac{1}{\omega} t. \quad (2.6)$$

Scaling the Navier–Stokes equation (2.1) and continuity equation (2.2) in this way leads to

$$\beta \left(\frac{\partial}{\partial t} \mathbf{u} + \alpha \mathbf{u} \cdot \nabla \mathbf{u} \right) = -\nabla p + \nabla^2 \mathbf{u}, \quad (2.7)$$

$$\nabla \cdot \mathbf{u} = 0. \quad (2.8)$$

There are two dimensionless numbers in the scaled Navier–Stokes equation, denoted α and β . This is due to the presence of two separate time scales, h/A and $1/\omega$, within the system. The former constitutes the convective time scale, while the latter constitutes the diffusive time scale. The parameter β is referred to as the Stokes number, and relates to the rate of diffusion of vorticity within the flow. The parameter α is effectively a measure of the relative importance of convection within

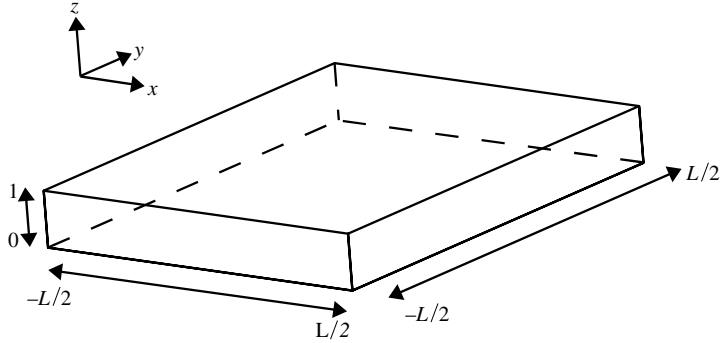


FIGURE 2. Diagram of the channel domain, in scaled coordinates. We consider an infinite channel in which $L \rightarrow \infty$. Because of the inherent symmetry of the flow, we may neglect the spanwise (or y) dimension.

the system. The values of these parameters are given by

$$\alpha = \frac{A}{h\omega}, \quad \beta = \frac{\rho h^2 \omega}{\mu}. \quad (2.9)$$

If we define a Reynolds number based upon the amplitude of the boundary condition by

$$Re = \frac{\rho h A}{\mu}, \quad (2.10)$$

then we may also express α as a ratio of dimensionless numbers:

$$\alpha = \frac{Re}{\beta}. \quad (2.11)$$

The scaled domain of the flow, equivalent to (2.3), is given by

$$-\infty < x < \infty, \quad 0 \leq z \leq 1. \quad (2.12)$$

A diagram of the domain of the flow, in scaled variables, is shown in figure 2.

In scaled variables, the boundary conditions defined in (2.4) become

$$w = \begin{cases} \sin(\eta x + t), & \text{at } z = 1, \\ \gamma \sin(\eta x + t - \phi), & \text{at } z = 0. \end{cases} \quad (2.13)$$

A new dimensionless parameter, η , appears in these dimensionless boundary conditions. It represents the ratio of the height of the channel to the wavelength of the sinusoidal waves defining the boundary conditions, and is formally defined as

$$\eta = \frac{h}{\lambda}. \quad (2.14)$$

Since the no-slip boundary condition applies to the flow in the streamwise direction, we have

$$u = 0 \quad \text{at } z = 0, 1. \quad (2.15)$$

2.3. Averaging

For all quantities, wall-parallel averages are denoted by an overbar and are defined as

$$\bar{F}(z, t) \stackrel{\text{def}}{=} \lim_{L \rightarrow \infty} \frac{1}{L} \int_{-L/2}^{L/2} F(\mathbf{x}, t) \, dx. \tag{2.16}$$

A non-zero wall-parallel average of the streamwise velocity, $\bar{u}(z, t)$, is referred to here as a ‘translational’ flow. This concept is introduced here as a mathematical convenience. Use will be made of it in §4 and in appendix A. Fluctuations of quantities (by which we mean here any deviation in the value of a quantity from its wall-parallel average) are denoted by a prime and are defined as

$$F'(\mathbf{x}, t) \stackrel{\text{def}}{=} F(\mathbf{x}, t) - \bar{F}(z, t). \tag{2.17}$$

An average over the entire channel is denoted by angled brackets and is defined as

$$\langle F(t) \rangle \stackrel{\text{def}}{=} \int_0^1 \bar{F}(z, t) \, dz. \tag{2.18}$$

In dimensional variables, the wall-parallel averages of quantities are mathematically defined in an identical manner to their equivalents in scaled variables. The average over the entire channel, however, is defined differently, owing to its dependence upon h , the height of the channel. In terms of dimensional variables, (2.18) is equivalent to

$$\langle \hat{F}(\hat{t}) \rangle \stackrel{\text{def}}{=} \frac{1}{h} \int_0^h \hat{F}(\hat{z}, \hat{t}) \, d\hat{z}. \tag{2.19}$$

For the non-dimensionalised velocity, $\langle u \rangle$ can denote either the average streamwise velocity within the channel, or the volume flux through the channel (henceforth referred to as the ‘bulk flow’). However, for the dimensionalised velocity, $\langle \hat{u} \rangle$ denotes exclusively the average velocity, and must be multiplied by h to obtain the bulk flow.

2.4. Streamfunction

Because the flow is two-dimensional, we can express the velocity in terms of a streamfunction $\Psi(\mathbf{x}, t)$. In this formulation, the streamwise, u , and wall-normal, w , components of the velocity vector are given by

$$u = \frac{\partial \Psi}{\partial z}, \quad w = -\frac{\partial \Psi}{\partial x}. \tag{2.20}$$

By taking the curl of the Navier–Stokes equation, and substituting the streamfunction for the fluid’s velocity, we obtain the evolution equation for $\Psi(\mathbf{x}, t)$ as

$$\beta \frac{\partial}{\partial t} \nabla^2 \Psi + \alpha \beta \left(\frac{\partial \Psi}{\partial z} \frac{\partial}{\partial x} - \frac{\partial \Psi}{\partial x} \frac{\partial}{\partial z} \right) \nabla^2 \Psi = \nabla^4 \Psi. \tag{2.21}$$

3. Perturbation analysis for boundary conditions of small amplitude

Within this section, we describe the methodology we have used to determine the properties of the flow. We analyse flows driven by transpiration through a perturbation analysis for small values of the perturbation parameter α . An outline of the derivation and the results are presented within this section. The full derivation is found in appendix A.

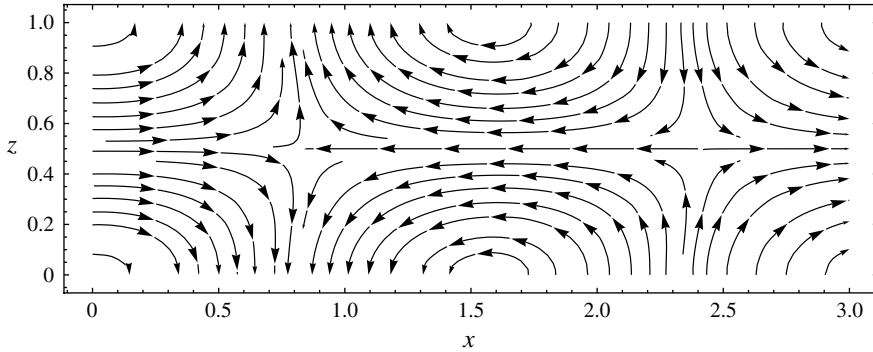


FIGURE 3. Plot of instantaneous streamlines of $\mathbf{u}_0(\mathbf{x}, t)$, the leading-order approximation of the flow for $\beta = 20$ and $\eta = 2$, using an antiphase boundary condition ($\gamma = 1$, $\phi = \pi$).

The method involves expanding the velocity, streamfunction and pressure in terms of α , as follows:

$$\mathbf{u} = \mathbf{u}_0 + \alpha \mathbf{u}_1 + \alpha^2 \mathbf{u}_2 + \alpha^3 \mathbf{u}_3 + \dots, \quad (3.1a)$$

$$\Psi = \Psi_0 + \alpha \Psi_1 + \alpha^2 \Psi_2 + \alpha^3 \Psi_3 + \dots, \quad (3.1b)$$

$$p = p_0 + \alpha p_1 + \alpha^2 p_2 + \alpha^3 p_3 + \dots. \quad (3.1c)$$

Further details of the perturbation methodology are given in appendix A.1.

3.1. Leading-order flow

The leading-order term $\mathbf{u}_0(\mathbf{x}, t)$ represents a Stokes flow subject to transpiration boundary conditions. Its derivation can be found in appendix A.2. The leading-order streamfunction, also found in (A 14), is given by

$$\begin{aligned} \Psi_0 = & \left(c_1 e^{\eta z} + c_2 e^{-\eta z} + c_3 e^{\sqrt{\eta^2 + \beta i z}} + c_4 e^{-\sqrt{\eta^2 + \beta i z}} \right) e^{i(\eta x + t)} \\ & + \left(c_1^* e^{\eta z} + c_2^* e^{-\eta z} + c_3^* e^{\sqrt{\eta^2 - \beta i z}} + c_4^* e^{-\sqrt{\eta^2 - \beta i z}} \right) e^{-i(\eta x + t)}, \end{aligned} \quad (3.2)$$

where the various constants c_1, c_1^* , etc. depend upon β, η, γ and ϕ , and are given in (A 12) of appendix A. Despite containing several complex terms, the above function for Ψ_0 is in fact real for all applicable values of the parameters β, η, γ and ϕ . A vector plot of an instantaneous realization of the leading-order flow, from an antiphase boundary condition, can be seen in figure 3. Regardless of the values of β and η , all such leading-order vector plots have the same general appearance.

3.2. First-order correction to the flow

The first-order correction to the bulk flow, $\langle u_1 \rangle$, is derived in appendix A.3. The closed forms for \bar{u}_1 and $\langle u_1 \rangle$ can be found in (A 24) and (A 25) respectively. Owing to their complexity, these are left to appendix A. Plots of $\langle u_1 \rangle / \beta$ can be seen in figures 4, 5 and 6. Here we have plotted $\langle u_1 \rangle / \beta$, rather than $\langle u_1 \rangle$, since we are most interested in determining the bulk flow induced for a particular amplitude of the boundary condition (that is, for a particular Re). From the definition of the convection parameter α , given in (2.11), we can see that an expansion of the velocity in α must be divided by β to become the equivalent expansion in Re .

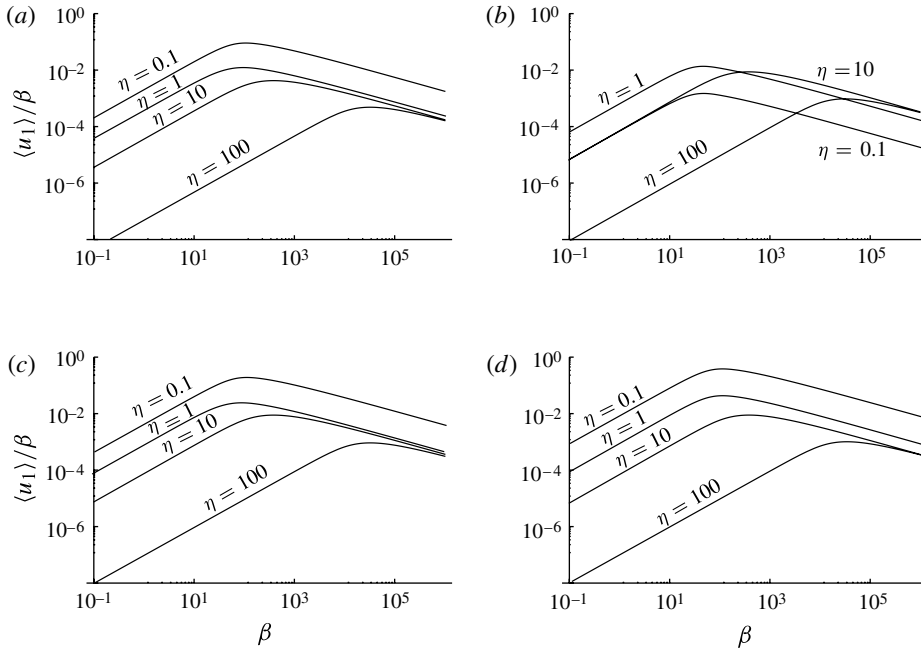


FIGURE 4. Log–log plots of $\langle u_1 \rangle / \beta$ against the Stokes number, $\beta = \rho h^2 \omega / \mu$, for several values of the ratio of the channel height to the boundary condition wavelength, $\eta = h / \lambda$: (a) ‘mixed’ boundary conditions; (b) in-phase boundary conditions; (c) out-of-phase boundary conditions; and (d) antiphase boundary conditions.

If we were to plot $\langle u_1 \rangle$, we would find that it increases monotonically with the Stokes number, β , potentially giving the misleading impression that increasing β invariably increases the induced bulk flow. This is, however, an illusion caused by the fact that increasing β while holding α constant implies commensurately increasing Re .

We are able to approximate the bulk flow induced via transpiration as

$$\langle u \rangle = \alpha \langle u_1 \rangle + O(\alpha^3). \tag{3.3}$$

Note that the error term in the above equation is of order α^3 . It can easily be verified that the next-order term in the velocity expansion, $\mathbf{u}_2(\mathbf{x}, t)$, contains only swirling, rather than translational, flow, by substituting (A 5) and (A 17) into (A 1c). (In their analysis of flows driven solely by transpiration, Min *et al.* (2006) employed values of α ranging from $\alpha = 0.0025$ to $\alpha = 0.075$.)

Equation (3.3) appears to imply that the bulk flow increases linearly with the amplitude of the boundary condition, A . However, it is important to note that, because the velocity has been scaled via A , as defined in (2.6), the dimensional velocity will in fact be proportional to A^2 .

The derivation of the remaining components of the first-order correction to the flow field is given in appendix A.4.

3.3. Boundary conditions of long wavelength

In all results except the in-phase case, it can be clearly seen that $\langle u_1 \rangle$ is maximized by minimizing η (the ratio of the channel height to the wavelength of the boundary

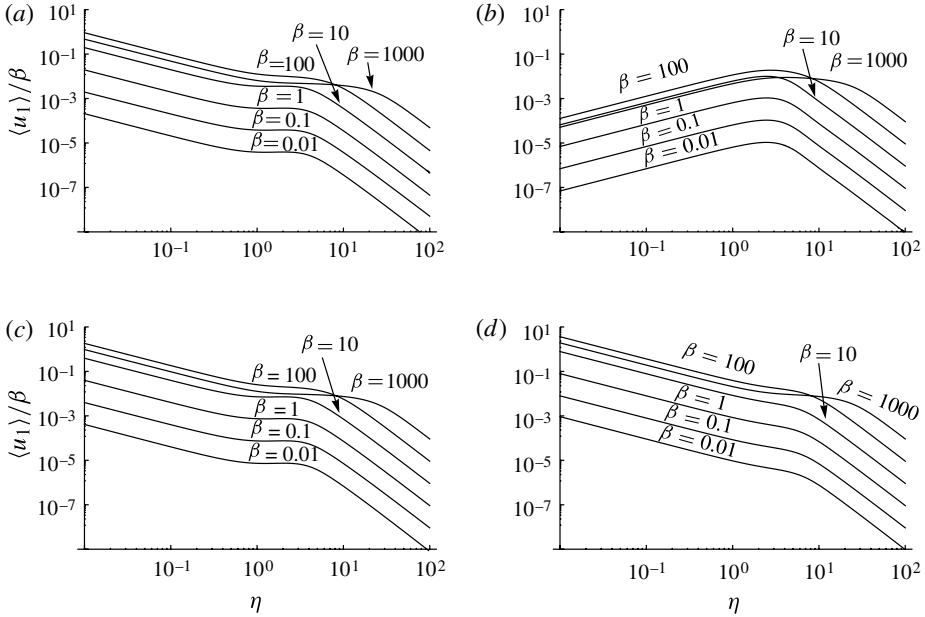


FIGURE 5. Log–log plots of $\langle u_1 \rangle / \beta$ against η ($= h/\lambda$) for several values of β ($= \rho h^2 \omega / \mu$): (a) ‘mixed’ boundary conditions; (b) in-phase boundary conditions; (c) out-of-phase boundary conditions; and (d) antiphase boundary conditions.

condition). The asymptotic behaviour of $\langle u_1 \rangle$ in the small- η limit is given by

$$\langle u_1 \rangle \sim \frac{\gamma^2 - 2\gamma \cos \phi + 1}{\eta} f_1(\beta), \tag{3.4}$$

where

$$\begin{aligned} f_1(\beta) \equiv & \left\{ \beta(10 - i\beta) \sinh\left(\frac{\sqrt{-i\beta}}{2}\right) \cosh\left(\frac{\sqrt{i\beta}}{2}\right) \right. \\ & \left. + \cosh\left(\frac{\sqrt{-i\beta}}{2}\right) \beta \left[(\beta - 10i) \sinh\left(\frac{\sqrt{i\beta}}{2}\right) + 10i\sqrt{i\beta} \cosh\left(\frac{\sqrt{i\beta}}{2}\right) \right] \right\} \\ & \times \sinh\left(\frac{\sqrt{-i\beta}}{2}\right) \sinh\left(\frac{\sqrt{i\beta}}{2}\right) \left\{ 2 \left[-\sqrt{i\beta} \sinh\left(\sqrt{i\beta}\right) + 2 \cosh\left(\sqrt{i\beta}\right) - 2 \right] \right. \\ & \left. \times \left[-2\sqrt{-i\beta} + i\beta \sinh\left(\sqrt{-i\beta}\right) + 2\sqrt{-i\beta} \cosh\left(\sqrt{-i\beta}\right) \right] \right\}^{-1}. \end{aligned} \tag{3.5}$$

The above equation clearly demonstrates that the antiphase boundary condition induces the greatest bulk flow for $\eta < 1$. This concurs with the findings of Mamori *et al.* (2010), who reported that the antiphase boundary condition produced significantly greater drag reduction than the in-phase case, for an upstream-travelling wave acting upon a laminar Poiseuille flow.

By inspection of figures 5 and 6, it can be verified that (3.4) is a good approximation, in the ‘mixed’, out-of-phase and antiphase cases, for values of η less than unity (in other words, all systems in which the wavelength of the boundary condition is greater than the height of the channel). In fact, it is a good approximation, at such values of η , for all boundary conditions, except for those that are similar to

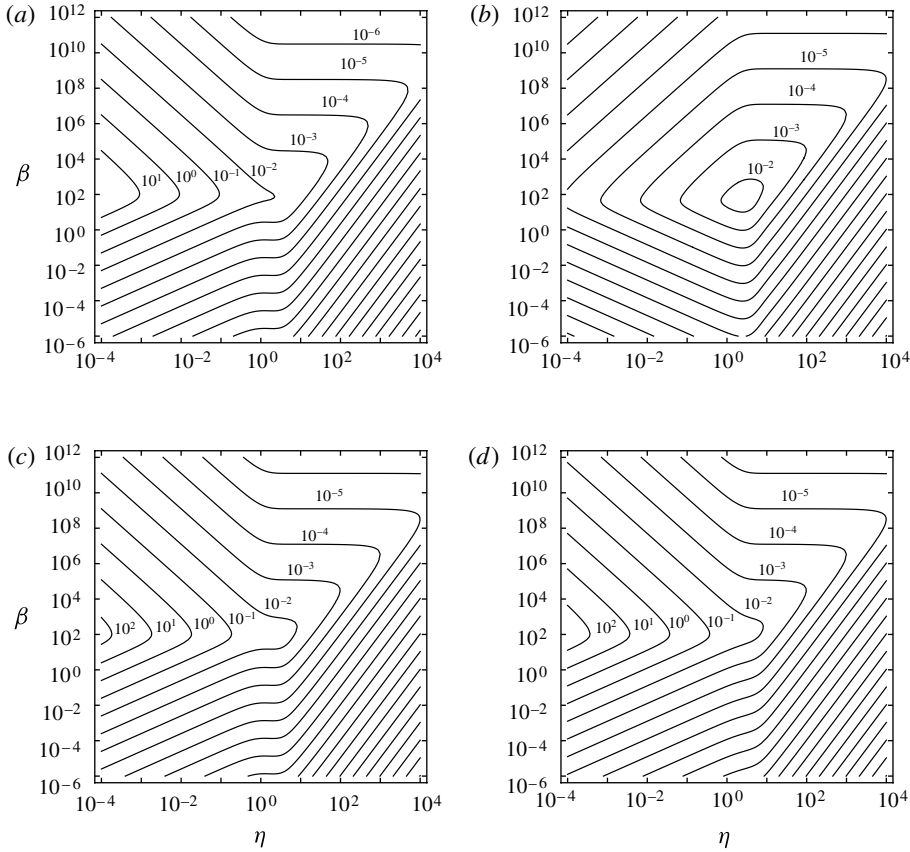


FIGURE 6. Contour plots of $\langle u_1 \rangle / \beta$ against β ($= \rho h^2 \omega / \mu$) and η ($= h / \lambda$): (a) ‘mixed’ boundary conditions; (b) in-phase boundary conditions; (c) out-of-phase boundary conditions; and (d) antiphase boundary conditions.

the in-phase case (i.e. those in which $2\gamma \cos \phi - \gamma^2 \approx 1$). If we further consider the limiting cases in which the Stokes number, β , approaches zero or infinity, we find that

$$\langle u_1 \rangle \sim \begin{cases} \frac{1 + \gamma^2 - 2\gamma \cos \phi}{5040} \frac{\beta^2}{\eta}, & \eta \rightarrow 0, \beta \rightarrow 0, \\ \frac{1 + \gamma^2 - 2\gamma \cos \phi}{2\sqrt{2}} \frac{\sqrt{\beta}}{\eta}, & \eta \rightarrow 0, \beta \rightarrow \infty. \end{cases} \quad (3.6)$$

From (3.4) it can be determined that the optimal value of β (i.e. that which maximises $\langle u_1 \rangle / \beta$) is given by

$$\beta_{max} \approx 107. \quad (3.7)$$

This of course implies that there exists an optimal frequency, beyond which any further increase to the frequency will result in a reduced bulk flow. This concurs with previous findings by Min *et al.* (2006), Hoepffner & Fukagata (2009), Mamori *et al.* (2010) and Moarref & Jovanović (2010).

It might be expected that the ‘mixed’ boundary condition should always induce the least bulk flow, since it involves transpiration acting at only one wall. However, while

it does invariably induce less bulk flow than the out-of-phase and antiphase cases, it can be clearly seen that, for $\eta < 1$, it is by far the in-phase case that is the least effective in inducing a bulk flow. The reason for this is that to reduce η is equivalent to reducing the height of the channel (it follows from the definition of η that this is also equivalent to increasing the wavelength of the boundary conditions). Because the velocity gradients at either wall are defined to be equal in the in-phase case, a short channel contains very little space for velocity gradients to develop, within the fluid. Where the velocity gradients are small, the effect of convection will also be small.

3.4. Boundary conditions of short wavelength

The flow is qualitatively different at large η , where the height of the channel is significantly greater than the wavelength of the boundary condition. If we consider the limiting case in which $\eta \rightarrow \infty$, it is clear, by inspection of (A 12), that in this limit, all of c_1, c_1^*, \dots , are zero for all varieties of boundary conditions. From this, we may infer that, for all boundary conditions,

$$\lim_{\eta \rightarrow \infty} \langle u \rangle = 0. \quad (3.8)$$

This is an intuitive result, since the greater the relative height of the channel to the wavelength of the boundary condition, the more likely it is that at any point within the flow, the effects of the adjacent peaks and troughs of the boundary condition will combine, resulting in a flow containing only small velocity gradients.

Similarly, as η increases, the dependence of $\langle u_1 \rangle$ upon the phase difference, ϕ , generally decreases. By inspection, it is clear that, for values of η greater than around 10, the bulk flow is effectively independent of ϕ . This is due to the fact that, as the height of the channel increases, the effect of the boundary condition at one wall upon the flow near to the opposite wall decreases. As a result, the effect of the phase difference becomes negligible in the large- η limit. The asymptotic behaviour of the bulk flow in this large- η limit is given by

$$\langle u_1 \rangle \sim \begin{cases} \frac{3(1 + \gamma^2) \beta^2}{64 \eta^3}, & \eta \rightarrow \infty, \frac{\beta}{\eta^2} \rightarrow 0 \\ \frac{1 + \gamma^2}{4\sqrt{2}} \sqrt{\beta}, & \eta \rightarrow \infty, \frac{\beta}{\eta^2} \rightarrow \infty. \end{cases} \quad (3.9)$$

3.5. Dependence on the frequency of oscillation

The Stokes number, β , defined in (2.9), is proportional to the frequency of oscillation of the boundary condition. Hence, by considering the effect of β upon $\langle u_1 \rangle / \beta$, we can see the effect of the frequency upon the bulk flow.

Plots of the first-order correction to the flow, $\langle u_1 \rangle / \beta$, for $\eta = 2$, can be seen in figure 7. There it can be clearly seen that, for $\beta < 1$, the first-order correction to the flow tends to consist largely of swirling, rather than translational, motion, while for $\beta > 1$, the first-order flow is primarily translational. In fact, even for very large values of β , the swirling motions within the first-order correction are negligible in comparison to the streamwise translational motion. This is despite the fact that, as can be seen in figure 4, the translational motion is itself minute at such values of β .

In fact, a notable result is found in the limit as $\beta \rightarrow \infty$, with Re held constant. This corresponds to a system in which the boundary condition is travelling very rapidly

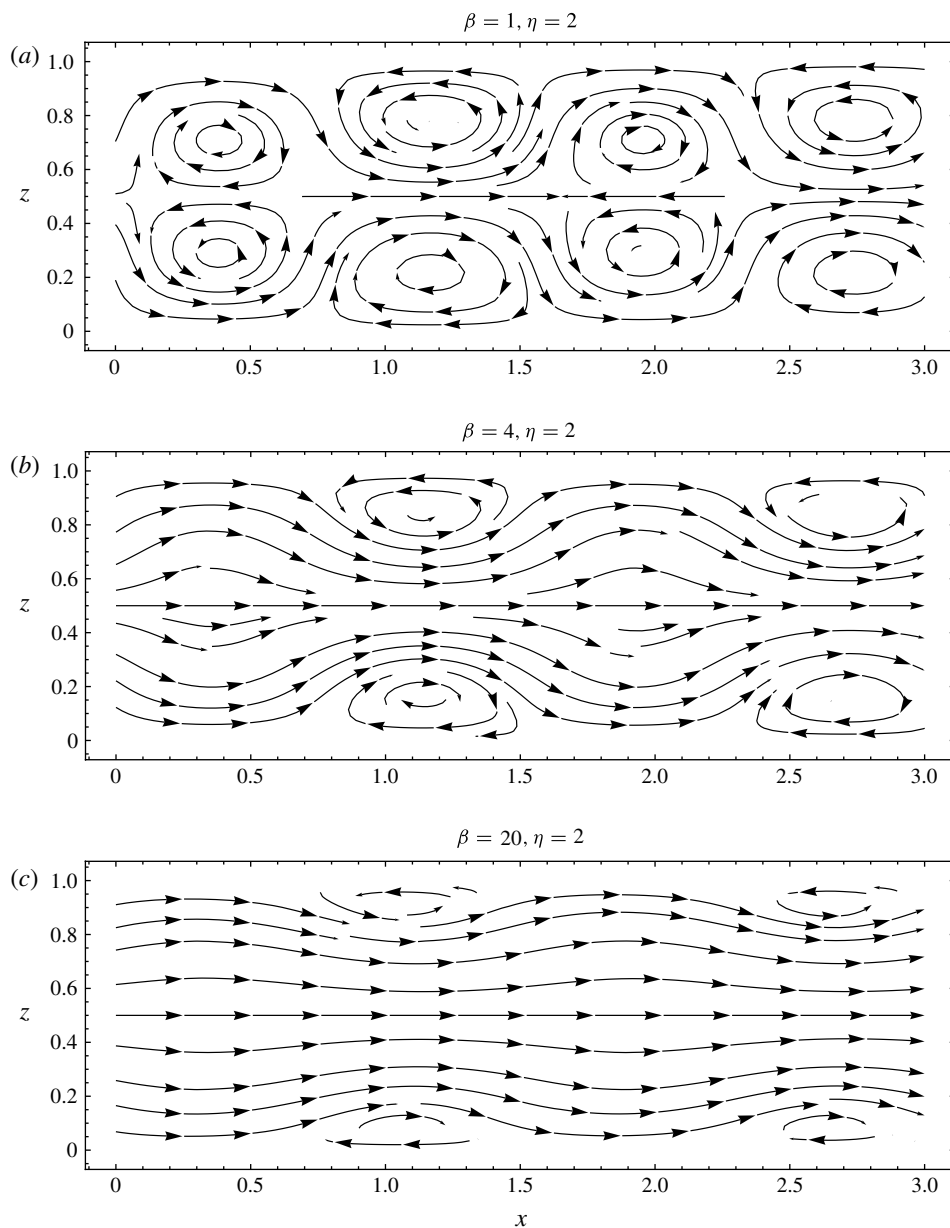


FIGURE 7. Plots of instantaneous streamlines of $\mathbf{u}_1(\mathbf{x}, t)/\beta$, the first-order correction of the flow for $\eta = 2$ and several values of β , using an antiphase boundary condition ($\gamma = 1, \phi = \pi$).

along the wall of the channel. In this limit, the streamfunction asymptotes to

$$\Psi \sim \frac{\text{csch } \eta}{\eta} [\sinh(\eta z) \cos(\eta x + t) + \gamma \sinh(\eta(1 - z)) \cos(\eta x + t - \phi)]$$

as $\beta \rightarrow \infty$. (3.10)

Note that the above equation contains the total streamfunction, $\Psi(\mathbf{x}, t)$, rather than merely its leading-order term, $\Psi_0(\mathbf{x}, t)$. This conclusive result follows from the fact

that, in this limit, the constants c_3 , c_3^* , c_4 and c_4^* are zero. In fact, they approach zero sufficiently rapidly that the right-hand side of (A 23) is zero. By inspection of (A 25), it is clear that this implies that

$$\lim_{\beta \rightarrow \infty} \langle u \rangle = 0, \quad Re = \text{constant}. \quad (3.11)$$

They also approach zero sufficiently rapidly that

$$\Psi_1(\mathbf{x}, t) = 0. \quad (3.12)$$

It is clear from (A 1c) and the perturbation methodology that in this limit

$$\Psi_n(\mathbf{x}, t) = 0 \quad \text{for all } n > 0. \quad (3.13)$$

In other words, as β dominates Re , the effect of convection becomes negligible, and the entire flow will be of the same streamwise scale of motion as the boundary condition. (In this sense, the flow at large β resembles the flow at small Re .)

The most notable aspect of (3.10) is that it does not satisfy the no-slip boundary condition (2.15). It may appear a paradoxical result that the solution to the Navier–Stokes and continuity equations, subject to transpiration, asymptotes towards a velocity field that does not satisfy its own boundary conditions. This result can be explained, however, by analogy with the motion of a fluid of low viscosity adjacent to an oscillating body (Stokes 1851). In such flows, a thin vorticity-containing boundary layer is known to form, the thickness of which decreases as the frequency of oscillation increases.

Similarly, in the case of transpiration, an irrotational region forms within the centre of the channel at high β . The reason for this is that, as β increases, the vorticity generated by the adjacent peaks and troughs of the boundary condition begins to cancel away from the wall. This results in vorticity being confined to thin regions near to the walls. As β increases further, these vorticity-containing boundary layers decrease in width, approaching an infinitesimal width in the limit as $\beta \rightarrow \infty$. (Indeed, by inspection, it is clear that the flow represented by (3.10) is in fact entirely irrotational.) It is for this reason that the limiting behaviour of the flow as $\beta \rightarrow \infty$ does not satisfy its own boundary conditions.

In the case of high- Re flows, however, no such irrotational region forms. This is because the transpiration boundary condition causes vorticity to be convected away from the wall towards the centre of the channel. The system is therefore not reliant upon diffusion to spread vorticity from the near-wall region to the centre of the channel at high Re . We discuss the case of flows at high Re further in § 5.

3.6. Generalized boundary conditions

It may appear that the family of boundary conditions that have been defined by (2.13) constitute a significant restriction upon the analysis presented in this work. However, as we demonstrate in this section, these results can be readily extended to any channel flow for which the functions defining w at the walls can be expressed as convergent Fourier series in $\eta x + t$.

In order to explain how these results can be extended, it is necessary to formally define what we call *streamwise scales of motion*. Since the flow field is periodic in the x direction, and with respect to time, the entire flow field can be expressed as a Fourier series in $\eta x + t$. Each component of that Fourier series will be referred to as a streamwise scale of motion (these could alternatively be called Fourier modes in $\eta x + t$). For example, (A 5) indicates that $\Psi_0(\mathbf{x}, t)$ contains just one streamwise scale of motion,

which is equal to that of the boundary condition, while (A 16) indicates that $\Psi_1(x, t)$ contains two scales of motion. One of these scales has half the wavelength of the boundary condition, and the other is *translational*, by which we mean that it is not periodic in $\eta x + t$.

Fundamental to the method of extending these results is the observation that it is only the convection of each scale of motion at leading order by itself that can produce a translational flow at first order. Only at second order or higher may two different streamwise scales of motion produce a translational flow. The method of extending these results to more general boundary conditions consists of expanding the boundary conditions in a Fourier series in order to re-express them as a sum of functions, each of which satisfies (2.13), with appropriate substitutions for β , η , γ and ϕ .

Hence, if we define a new function $\mathcal{U}(\beta, \eta, \gamma, \phi)$ to be the first-order bulk flow for a specific set of the flow parameters, so that

$$\mathcal{U}(\beta', \eta', \gamma', \phi') \stackrel{\text{def}}{=} \langle u_1 \rangle, \quad \beta = \beta', \quad \eta = \eta', \quad \gamma = \gamma', \quad \phi = \phi', \quad (3.14)$$

it follows that, if the boundary condition can be expressed as

$$w = \begin{cases} \sum_{n=0}^{\infty} A_n \sin n(\eta x + t), & \text{at } z = 1, \\ \sum_{n=0}^{\infty} A_n \gamma_n \sin n(\eta x + t - \phi_n), & \text{at } z = 0, \end{cases} \quad (3.15)$$

where the A_n are constants, then the bulk flow at first order can be expressed as

$$\langle u_1 \rangle = \sum_{n=0}^{\infty} \frac{A_n}{n} \mathcal{U}(n\beta, n\eta, \gamma_n, \phi_n). \quad (3.16)$$

For flows at low η , it should significantly reduce the complexity of the resulting function to define \mathcal{U} in terms of the low- η asymptote given in (3.4).

Note that there is a factor of $1/n$ in the above equation, which results from (3.3), and the dependence of α upon β . In scaling the Navier–Stokes equation, the characteristic velocity (equivalent to A in this study) should be chosen to be the highest of the amplitudes of the scales of motion that are present within the boundary conditions. In that way, it can be guaranteed that, for all n , we will have $0 \leq A_n \leq 1$. The uncertainty involved in this extended derivation will be either $O(\alpha^2)$ or $O(\alpha^3)$, depending on the scales of motion present within the boundary conditions.

The summation in (3.16) should converge, assuming that the Fourier series that defines the boundary conditions converges. This is because $\langle u_1 \rangle$ approaches zero for high values of β and η . However, particularly at low values of β and η , the summation in (3.16) may contain a large number of non-negligible terms, and may therefore converge only very slowly.

While only a subset of all possible periodic boundary conditions can be expressed in the form of (3.15), this nonetheless suggests a practical method by which the bulk flow induced by any periodic wall-normal boundary conditions may be determined. This method involves first solving for a system whose boundary conditions take the form of

the combination of a sine wave and a cosine wave at both walls; for example,

$$w = \begin{cases} \sin(\eta x + t) + \gamma \cos(\eta x + t), & \text{at } z = 1, \\ \delta \sin(\eta x + t) + \epsilon \cos(\eta x + t), & \text{at } z = 0, \end{cases} \quad (3.17)$$

where γ , δ and ϵ are constants between -1 and 1 . Then, $\langle u_1 \rangle$ could be determined for such a system via an analogous derivation to that by which $\langle u_1 \rangle$ has been determined in this work. It would be found that the leading-order streamfunction, $\Psi_0(\mathbf{x}, t)$, would still take the form of (3.2), with the exception that the constants c_1 , c_1^* , c_2 , etc. would take different values from those they have here, and would depend upon the parameters γ , δ and ϵ . Having rederived the values of c_1 , c_1^* , etc. in this way, the remainder of the derivation would proceed as before, and $\langle u_1 \rangle$ would again be given by (A 25).

Because any periodic function may be expanded as a Fourier series, it follows that, if we were to define a new function $\mathcal{W}(\beta, \eta, \gamma, \delta, \epsilon)$ in an equivalent manner to (3.14), and expand the boundary conditions in an analogous way to (3.15), the bulk flow could then be represented by the equivalent of (3.16).

4. Energy considerations

Marusic *et al.* (2007) considered the effect of transpiration in conjunction with an externally applied pressure gradient across the channel. They derived the conditions required for transpiration to produce sublaminal drag, in the presence of such an applied pressure gradient. Their formula relates the rate at which the transpiration imparts energy upon the flow to the rate at which energy is dissipated within the flow. They derived the rule that the drag will be sublaminal if and only if

$$\mathcal{W} > \langle |\nabla \mathbf{u}'|^2 \rangle + Re \langle (\overline{u'w'} - \langle u'w' \rangle)^2 \rangle, \quad (4.1)$$

where \mathcal{W} represents the rate at which energy is being imparted upon the flow via transpiration. It is given by

$$\mathcal{W} = \frac{1}{2} Re \overline{(w')^3 + w'p'} \Big|_{z=0} - \frac{1}{2} Re \overline{(w')^3 + w'p'} \Big|_{z=1}. \quad (4.2)$$

The $(1/2)(w')^3$ term represents the overall rate at which energy is input (or removed) as kinetic energy, while the $w'p'$ term represents the overall rate at which energy is transferred by flowing against (or with) a local pressure gradient. This notably excludes any energy that is imparted due to an overall cross-flow within the channel. The first term on the right-hand side of (4.1) represents the dissipation due to fluctuations within the flow (i.e. not counting dissipation due to the wall-parallel averaged flow). The $\overline{u'w'}$ term represents the Reynolds shear stress (which is the stress acting upon the wall-parallel averaged flow due to the presence of the fluctuations).

There are factors of Re in (4.1) and (4.2) above that are absent from the equivalent equations in the work by Marusic *et al.* (2007). These result from the fact that a different scaling has been employed in this work. The scaling used in this section is the same as that in § 3.

It must be stressed, however, that (4.1) applies strictly to those flows in which the applied pressure gradient across the channel is non-zero. The systems we have considered in this work all have no such applied pressure gradients. The equivalent equation for a flow in the absence of an applied pressure gradient or an overall cross-flow can be found by removing all of the terms relating to time derivatives,

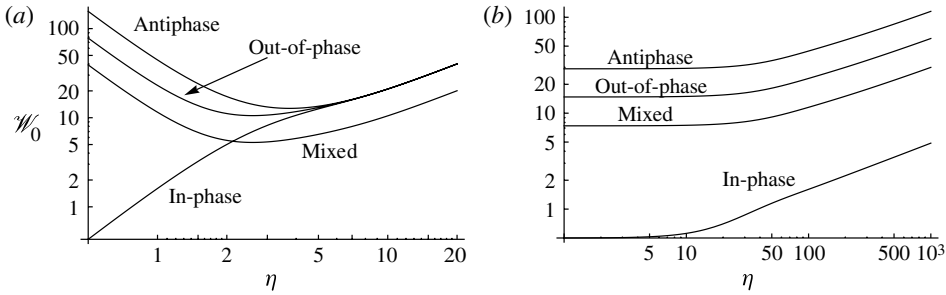


FIGURE 8. Log–log plots of \mathcal{W}_0 , the leading-order component of the rate at which energy is being supplied to the flow, against β and η : (a) plots for $\beta = 100$; (b) plots for $\eta = 1$.

pressure gradients or a cross-flow from equations (2.10) and (3.5) of Marusic *et al.* (2007), and combining the results. This leads to

$$\mathcal{W} = \langle |\nabla \mathbf{u}'|^2 \rangle + Re(\langle \overline{u'w'} - \langle u'w' \rangle \rangle^2). \quad (4.3)$$

The above equation applies to all such flows, regardless of whether or not the transpiration has induced a bulk flow. The reason for this discrepancy between pressure-driven and non-pressure-driven flows is that, if a pressure gradient is applied in the streamwise direction of the flow, then the bulk flow will be removing energy from the system owing to the pressure difference between the inlet and outlet of the channel. This removal of energy must be accounted for within the flow’s overall energy balance, and therefore flows that are subject to an applied pressure gradient are fundamentally different from flows in which the inlet and outlet are at equal pressure.

It should be noted also that, for all of the flows investigated herein, the overall kinetic transfer, $(1/2) \langle w' \rangle^3$, at either wall will be zero. The driving energy of the flow therefore derives solely from the $w'p'$ term.

4.1. Energy input

We can now determine the rate at which transpiration imparts energy upon the flow by substituting (A 15), for the leading order of the pressure, into (4.2). This results in

$$\mathcal{W} = \underbrace{\frac{\beta}{2i} [\gamma(c_1 - c_2) e^{i\phi} + \gamma(c_2^* - c_1^*) e^{-i\phi} + (c_1^* e^\eta - c_2^* e^{-\eta}) + c_2 e^{-\eta} - c_1 e^\eta]}_{\mathcal{W}_0} + O(\alpha^2). \quad (4.4)$$

The first term on the right-hand side is the leading-order contribution to \mathcal{W} , and will henceforth be denoted by \mathcal{W}_0 . That there is no first-order correction to \mathcal{W} is clear from the streamwise scales of motion that are present at first order. Plots of \mathcal{W}_0 against β and η can be found in figure 8.

For values of η less than 1 (i.e. for systems in which the wavelength of the boundary condition is greater than the height of the channel), \mathcal{W}_0 increases as η decreases in all but the in-phase case. This is to be expected, since the induced bulk flow also increases as η decreases, at such values of η . The asymptotic behaviour of \mathcal{W}_0 , in the small- η limit, is given by

$$\mathcal{W}_0 \sim \frac{\gamma^2 - 2\gamma \cos \phi + 1}{\eta^2} f_2(\beta), \quad (4.5)$$

where

$$\begin{aligned}
 f_2(\beta) \equiv & \beta^2 \left[\sinh \left(\frac{\sqrt{-i\beta}}{2} \right) \cosh \left(\frac{\sqrt{i\beta}}{2} \right) + i \sinh \left(\frac{\sqrt{i\beta}}{2} \right) \cosh \left(\frac{\sqrt{-i\beta}}{2} \right) \right] \\
 & \times \left\{ 2 \left[\sqrt{i\beta} \cosh \left(\frac{\sqrt{i\beta}}{2} \right) - 2 \sinh \left(\frac{\sqrt{i\beta}}{2} \right) \right] \right. \\
 & \left. \times \left[2(-1)^{1/4} \sqrt{\beta} \sinh \left(\frac{1}{2}(-1)^{3/4} \sqrt{\beta} \right) + \beta \cosh \left(\frac{\sqrt{-i\beta}}{2} \right) \right] \right\}^{-1}. \quad (4.6)
 \end{aligned}$$

If we compare the above to (3.4), for the asymptotic behaviour of $\langle u_1 \rangle$ in the low- η limit, we find that, although the bulk flow is maximized by minimizing η , the energy cost of producing that flow increases at an even greater rate. We therefore have a diminishing return, in terms of induced bulk flow, for the energy input, as we increase the wavelength of the boundary condition. Moarref & Jovanović (2010), in their studies of Poiseuille flows subjected to transpiration, also found that transpiration became less energy-efficient at longer wavelength, despite the fact that the drag reduction induced by transpiration increases with the wavelength. They also similarly found that the energy cost increases with the frequency of the boundary condition (or equivalently with β), despite the fact that the induced bulk flow is negligible at large β .

Also noteworthy is the fact that, at high η and at high β , \mathscr{W}_0 is large. This is despite the fact that, at such values of η and β , the bulk flow induced is negligible. This has also been found to be true for Poiseuille flows subjected to transpiration, in the work by Moarref & Jovanović (2010).

5. Boundary conditions of large amplitude

In this section, we consider flows in which the maximum amplitude of the wall-normal velocity at the boundaries is very high in comparison to the speed at which the boundary condition moves along the wall of the channel. Specifically, we consider the mathematical limit as $\lambda\omega/A \rightarrow 0$, under the assumption that the flow remains two-dimensional. These amount to flows in which the effect of the time derivative is negligible in comparison to that of convection. Although transpiration at large amplitude has been found to be very energy-inefficient, and therefore of little practical use (Moarref & Jovanović 2010), it is considered here from a theoretical perspective for completeness.

We show that, in the limit as $\lambda\omega/A \rightarrow 0$, the bulk flow induced will become independent of A , depending instead only upon $\lambda\omega$ (the speed of the boundary condition).

In this section, the Navier–Stokes equation is written

$$Re_{\lambda\omega} \frac{\partial}{\partial t} \mathbf{u} + Re_A \mathbf{u} \cdot \nabla \mathbf{u} = -Re_A \nabla p + \nabla^2 \mathbf{u}. \quad (5.1)$$

The continuity equation (2.8) applies as before. A different scaling has been employed here from that used in the preceding sections. The reason for the change of scaling is because we will subsequently make use of a change of the inertial reference frame from which the flow is observed, and it is therefore preferable that the scaling should be independent of the reference frame.

Here we have used as our length scale the wavelength of the boundary condition, λ , rather than the height of the channel, h . In this section, the variables within the

Navier–Stokes equation are scaled according to

$$\hat{x} = \lambda x, \quad \hat{u} = Au, \quad \hat{p} = \rho A^2 p, \quad \hat{t} = \frac{1}{\omega} t. \tag{5.2}$$

Equation (5.1) contains two different Reynolds numbers, Re_A and $Re_{\lambda\omega}$. Here Re_A is based upon the amplitude of the boundary condition, while $Re_{\lambda\omega}$ is based upon the speed at which the boundary condition moves along the channel. They have been defined as

$$Re_A = \frac{\rho \lambda A}{\mu}, \quad Re_{\lambda\omega} = \frac{\rho \lambda^2 \omega}{\mu}. \tag{5.3}$$

Notice that Re_A is analogous to the Reynolds number Re that has been used in the preceding sections, while $Re_{\lambda\omega}$ is analogous to β/η .

We consider again the same set of possible boundary conditions as before, those defined by (2.13) and (2.15). When scaled according to (5.2), these boundary conditions become

$$u = 0, \quad z = 0, \eta, \tag{5.4}$$

$$w = \begin{cases} \sin(x + t), & \text{at } z = \eta, \\ \gamma \sin(x + t - \phi), & \text{at } z = 0. \end{cases} \tag{5.5}$$

Here we introduce a new inertial reference frame defined such that the observer is travelling along the channel at the same speed and in the same direction as the boundary condition. If X denotes the streamwise position in this new reference frame, then it is given by

$$X = x + t. \tag{5.6}$$

A new position vector \mathbf{X} is introduced for use in this new reference frame. It is defined by

$$\mathbf{X} \stackrel{\text{def}}{=} (X, z). \tag{5.7}$$

The velocity in this new frame will be denoted by $\mathbf{U}(X, t)$. It has streamwise component U , and wall-normal component W . The boundary conditions in this new frame are given by

$$U = \frac{Re_{\lambda\omega}}{Re_A}, \quad z = 0, \eta, \tag{5.8}$$

$$W = \begin{cases} \sin X, & \text{at } z = \eta, \\ \gamma \sin(X - \phi), & \text{at } z = 0. \end{cases} \tag{5.9}$$

We shall denote the pressure within this new frame by P . It is clear that the relationship between the bulk flows in the two frames will be simply

$$\langle U \rangle - \langle u \rangle = \frac{Re_{\lambda\omega}}{Re_A} \equiv \frac{\lambda\omega}{A}. \tag{5.10}$$

We convert the Navier–Stokes equation to this new frame by substituting (5.6) into (5.1). This results in

$$Re_{\lambda\omega} \frac{\partial}{\partial X} \mathbf{U} + Re_A \mathbf{U} \cdot \tilde{\nabla} \mathbf{U} = -Re_A \tilde{\nabla} P + \tilde{\nabla}^2 \mathbf{U}, \tag{5.11}$$

where $\tilde{\nabla}$ is the gradient vector in the new frame, and is defined by

$$\tilde{\nabla} \stackrel{\text{def}}{=} \left(\frac{\partial}{\partial X}, \frac{\partial}{\partial z} \right). \quad (5.12)$$

It is therefore clear that, if Re_A is sufficiently greater than $Re_{\lambda\omega}$, the effect of convection will outweigh the effect of the time derivative in the Navier–Stokes equation. Moreover, we can see in (5.11) that the time derivative will be negligible if

$$Re_A \gg Re_{\lambda\omega}. \quad (5.13a)$$

The above equation is in fact a comparison of velocity scales, specifying that the maximum amplitude of the boundary condition should be much greater than the speed at which it travels along the wall of the channel. Indeed, in expressing the above dimensionless numbers in terms of the quantities through which they have been defined in (5.3), the above inequality becomes

$$A \gg \lambda\omega. \quad (5.13b)$$

We therefore expand $\mathbf{u}(\mathbf{x}, t)$ and $\mathbf{U}(X, t)$ as follows:

$$\mathbf{u} = \mathbf{u}_0 + \frac{\lambda\omega}{A} \mathbf{u}_1 + \left(\frac{\lambda\omega}{A} \right)^2 \mathbf{u}_2 + \dots, \quad (5.14a)$$

$$\mathbf{U} = \mathbf{U}_0 + \frac{\lambda\omega}{A} \mathbf{U}_1 + \left(\frac{\lambda\omega}{A} \right)^2 \mathbf{U}_2 + \dots. \quad (5.14b)$$

We expand the pressure in the same manner. By substituting the above into the Navier–Stokes equation (5.1), and equating coefficients of orders of $\lambda\omega/A$, we obtain

$$\mathbf{U}_0 \cdot \tilde{\nabla} \mathbf{U}_0 = -\tilde{\nabla} P_0 + \frac{1}{Re_A} \tilde{\nabla}^2 \mathbf{U}_0. \quad (5.15)$$

The viscous term survives, regardless of the magnitude of Re_A , owing to the necessity of having a region of low streamwise velocity adjacent to either wall, in order to satisfy the no-slip boundary condition. The boundary conditions acting upon $\mathbf{U}_0(X, t)$ are

$$U_0 = 0, \quad z = 0, \eta, \quad (5.16)$$

$$W_0 = \begin{cases} \sin X, & \text{at } z = \eta, \\ \gamma \sin(X - \phi), & \text{at } z = 0. \end{cases} \quad (5.17)$$

Clearly, therefore, the system in the limit as $\lambda\omega/A \rightarrow 0$ is mathematically equivalent to a flow in which the boundary condition is stationary. If we consider a system in which the boundary condition is stationary, then, as a result of the symmetry of such a system, there could be no bulk flow, since there would be no preferential direction in which it could flow. This implies simply that

$$\langle U_0 \rangle = 0. \quad (5.18)$$

The magnitude of the bulk flow, in the new frame, will therefore be of the same order as the second term in the expansion of $\mathbf{U}(X, t)$ given in (5.14b). We therefore conclude that

$$\langle U \rangle \leq O \left(\frac{\lambda\omega}{A} \right) \quad \text{as } \frac{\lambda\omega}{A} \rightarrow 0. \quad (5.19)$$

From the relationship between the bulk flows in the two frames, given in (5.10), we can therefore see that

$$\langle u \rangle \leq O\left(\frac{\lambda\omega}{A}\right) \quad \text{as } \frac{\lambda\omega}{A} \rightarrow 0. \quad (5.20)$$

The factor of A in the denominator above results from the velocity scaling, as defined in (5.2). In terms of the dimensional velocity, \hat{u} , this result becomes

$$\langle \hat{u} \rangle \leq O(\lambda\omega) \quad \text{as } \frac{\lambda\omega}{A} \rightarrow 0. \quad (5.21)$$

This proof is reliant upon there being a single unique solution to the Navier–Stokes equation, since otherwise there would be no need for the flow to have a preferential direction, and hence the symmetry argument used here would not hold. While there exists no accepted proof that the full three-dimensional Navier–Stokes equation exhibits a unique solution, the uniqueness of solutions for two-dimensional flows, for initial boundary value problems on bounded domains, has previously been shown by Ladyzhenskaya (1958, 1963). (That Ladyzhenskaya’s proof applies to problems defined on bounded domains does not prevent it from being applicable here, since, although the channel is of infinite length, it is periodic in the streamwise direction. By exploiting the periodicity of the system, therefore, the domain can be split into an infinite number of identical sub-domains, each of finite streamwise length.)

The importance of this proof, from a practical perspective, is that it shows that to increase A will not necessarily result in an increased bulk flow. We do not know whether there is in fact a non-zero bulk flow in this limit, or its direction. We have proved this for the family of boundary conditions that are defined by (2.13). However, since the proof relies upon the inherent symmetry of a sine wave, it cannot be easily extended to a more generalized set of boundary conditions. By inspection, there are two types of boundary conditions to which this proof can readily be extended. The first case is those in which the function defining the boundary condition at the bottom wall, $w^-(x, z, t)$, is related to its counterpart at the top wall, $w^+(x, z, t)$, via

$$w^+(x, z, t) = -w^-(-x + \phi, z, t). \quad (5.22)$$

Notice that the parameter ϕ has been included above to indicate that the two functions may be out of phase to some degree. The second case is those in which $w = 0$ at one wall and the boundary condition at the other wall is symmetric in the streamwise direction. In both cases, the boundary conditions must be independent of the spanwise location, in order that the flow should remain two-dimensional.

One possible explanation for the diminishing increase in the bulk flow with $Re_A/Re_{\lambda\omega}$ follows from the effect of convection upon the scales of motion present within the flow. As has been shown in §3, if the convection parameter α is small, only the larger scales of motion will be non-negligible. However, as α increases, so too will the relative magnitude of the smaller scales of motion. These smaller scales of motion subsist by drawing energy and momentum from the scales above them. The quantity $Re_A/Re_{\lambda\omega}$ defines the relative importance of convection within the flow, and hence is analogous to α , within the present scaling. It follows, therefore, that at high $Re_A/Re_{\lambda\omega}$, the momentum that is imparted to the flow via transpiration at the walls will be readily convected down to the smaller scales of motion.

As has been demonstrated in this work, the effect of convection can also be to produce motions of higher scale from motions of lower scale. However, the results presented herein also demonstrate that the larger the scale of motion of the boundary

condition (in other words, the lower the value of η), the greater will be its general tendency to transfer its momentum to a bulk flow. It is likely to be generally true that the smaller the scale of motion, the lesser the tendency for convection to transfer its momentum to a bulk flow. Hence, the increasing prevalence of the smaller scales of motion at high $Re_A/Re_{\lambda\omega}$ could potentially explain this result.

Notably, in (5.21), there is no dependence of the dimensional average streamwise velocity, $\langle \hat{u} \rangle$, upon the density or viscosity of the fluid. This can be explained by the fact that at high Re_A , the effect of viscosity, upon the larger scales of motion present within $U_0(X, t)$ becomes negligible. This is clear by inspection of (5.15). As a result, at high Re_A , energy is primarily drawn from the larger scales of motion by convection, rather than dissipation.

It is important to stress the limitations of the above proof. The proof relies upon the assumption that the flow remains two-dimensional. However, the stability of Poiseuille flows subjected to transpiration has been studied by Lee *et al.* (2008), who showed that an upstream-travelling wave boundary condition will reduce the stability of the flow. The same was reported by Moarref & Jovanović (2010), and in simulations by Lieu *et al.* (2010). From this, we can safely infer that, at sufficiently high Re_A , the flow becomes unstable, and will turn turbulent. Once the flow becomes turbulent, this proof no longer holds, since turbulent flows are three-dimensional. It is also possible that the flow could begin to exhibit three-dimensional laminar behaviour at some sub-turbulent value of Re_A .

Regardless of the shape of the function defining the wall-normal boundary condition, if the magnitude of that boundary condition is much greater than the speed at which it moves down the wall of the channel, then the system will effectively be governed by (5.15) and the effectively stationary boundary conditions given in (5.16) and (5.17). It seems likely, therefore, that such flows will, as the amplitude further increases, also begin to exhibit zero or negligible increases to their bulk flows. Equally, it may also be that non-symmetric (and also spanwise-dependent) boundary conditions will similarly find that their bulk flows will not increase with the magnitudes of their boundary conditions, beyond a certain point. We therefore pose the following conjecture.

For a flow that is driven by a zero net mass-flux blowing and suction over the no-slip channel walls (also known as transpiration), regardless of the shape of the function that defines the boundary condition, if the magnitude of that transpiration is sufficiently great, and sufficiently greater than the speed at which the boundary condition moves along the wall of the channel, the bulk flow will become dependent only upon the speed at which the boundary condition moves along the wall of the channel.

If it could be shown that the Navier–Stokes equation exhibited a unique solution in three dimensions, then this proof could be extended to three-dimensional flows driven by transpiration (provided that their boundary conditions were appropriately symmetric in the streamwise direction). Conversely, if the above conjecture could be shown to be incorrect for some such symmetric boundary conditions acting upon a three-dimensional flow, then it must follow that the Navier–Stokes equation does not in fact exhibit a unique solution in three dimensions. This we can infer from the previously stated fact that (5.15), subject to symmetric boundary conditions such as (5.16) and (5.17), could only induce a bulk flow if the Navier–Stokes equation were able to exhibit more than one solution.

6. Discussion

6.1. Scales of motion

The perturbation expansion presented within § 3 demonstrates the effect of convection upon the scales of motion present within the flow. In a Stokes flow, in which the effect of convection is absent or negligible, any separate streamwise scales of motion present will simply superimpose upon one another, without altering each other or giving rise to new scales of motion. (The exact meaning, in this work, of the term ‘scale of motion’ has been defined at the beginning of § 3.6.)

In inertial flows, however, convection acts to transfer energy and momentum from one scale of motion to another. In this example, the wavelength of the boundary condition forms a natural streamwise scale for the motion of the fluid within the channel. Naturally then, since the leading-order term in the perturbation expansion is an unsteady Stokes flow, the motion at leading order is of the scale of the boundary condition. At first order, however, two new streamwise scales arise due to the effect of convection: a series of eddies with a length scale half that of the boundary condition, and a translational flow, independent of the streamwise location.

If we were to extend our perturbation analysis (in the manner of Moarref & Jovanović 2010) to determine the second-order components of the flow, we would find that there exists at second order a scale of motion one-third the length of that of the boundary condition. As we pursue the analysis further, we would find that at the n th order, the expansion introduces a scale of motion $1/(n + 1)$ times the length of the scale of the boundary condition. Hence we can see that energy and momentum are drawn by each lesser scale of motion from the scales above it.

However, the translational flow is of a higher streamwise scale of motion than that of the boundary condition. The question of whether transpiration will be capable of inducing a non-zero bulk flow therefore becomes a question of whether the motion of the fluid may, under the influence of convection, provide energy and momentum to the translational flow from the lower scales of streamwise motion.

The analysis presented herein demonstrates that an inertial flow driven by transpiration will indeed experience such a transference of energy and momentum upwards in scale, to feed the translational motion of the fluid. Not only that, but an analysis of the higher-order terms within the perturbation expansion reveals that all scales of motion are drawing some of their energy from lower scales. This general tendency of energy to transfer downwards in scale is to be expected, since any upward transfer of energy requires that the scales of motion within the flow should combine in a coherent manner.

6.2. The induced bulk flow

The exact nature of the induced streamwise flow varies considerably with the geometry of the channel and the boundary conditions. However, certain general statements can be made about it: for example, the induced flow is invariably in what we have consequently referred to here as the streamwise direction, the direction counter to the motion of the boundary condition. This rule has been reported previously by Hoepffner & Fukagata (2009).

It might be expected that the in-phase boundary condition would produce a greater bulk flow than the ‘mixed’ boundary condition, since the in-phase boundary condition contains, in effect, twice the active flow control. However, as has been discussed in appendix A.3, this is only true for $\eta > 10$, or equivalently when the height of the channel is significantly greater than the wavelength of the boundary condition.

More revealing perhaps is the fact that, for $\eta < 1$ (where the wavelength of the boundary condition is longer than the height of the channel), the ‘mixed’ boundary condition induces a significantly higher bulk flow than the in-phase boundary condition. This can be attributed to the fact that the in-phase boundary condition sets an equal velocity at corresponding points on both walls, and thus reduces the velocity gradients within the flow, thereby decreasing the effect of convection. This will naturally be most noticeable at small η , where the ‘mixed’, out-of-phase or antiphase boundary conditions produce significant pressure and velocity gradients at the two walls, which are completely absent when an in-phase boundary condition is applied. This concurs with the findings of Mamori *et al.* (2010), who reported that the antiphase boundary condition produced significantly greater drag reduction for a Poiseuille channel flow than the in-phase boundary condition.

The justification for considering the out-of-phase mode separately from the antiphase mode is that the translational motion at first order results from the interaction of components of the leading-order flow that are out of phase by $\pi/2$. When ‘mixed’, in-phase or antiphase boundary conditions are employed, any leading-order flow that is out of phase with the boundary conditions by $\pi/2$ (that is, any flow whose streamfunction can be expressed as a multiple of $\sin(\eta x + t)$, where the boundary conditions are multiples of $\cos(\eta x + t)$) will result from the presence of the time derivative term within the Navier–Stokes equation. Thus the advantage of the out-of-phase boundary conditions is that since the flows at the two boundaries are out of phase by $\pi/2$, the presence of these two phases of the flow will not be dependent upon the time derivative. It follows that the out-of-phase mode could reasonably be expected to produce the greatest overall flow for sufficiently small values of the Stokes number, β .

However, the results show that the out-of-phase mode only generally induces a greater bulk flow than the antiphase flow for $\beta < 1$ and $1 < \eta < 10$, and, even in these cases, this difference is not significant. Moreover, at these values of β , the bulk flow induced by the transpiration is so small as to render these cases of little interest. For $\eta < 1$, the antiphase boundary condition produces the greatest bulk flow. We conclude, therefore, that the greater velocity gradients produced within the flow via the antiphase boundary conditions outweigh the reduced dependence upon the time derivative that is created by the out-of-phase boundary condition.

The antiphase mode produces the greatest bulk flow because it produces the greatest velocity gradients within the channel, and therefore should be the most affected by convection. This analysis suggests that an antiphase boundary condition should be considered as a flow-control regime for producing drag reduction, with a small η and a value for β of around 100.

The energy input required to support the system has been derived in § 4. Notably, for all except the in-phase case, the energy cost is proportional to η^{-2} for $\eta < 1$. This contrasts with the induced bulk flow, which has been shown to be proportional to η^{-1} in this limit. This tells us that, although it is possible to increase the induced bulk flow by increasing the wavelength of the boundary condition, by doing so an even greater increase in the power cost of the system will be incurred. A boundary condition of long wavelength will therefore not be the most energy-efficient method of driving a flow via transpiration. This is in agreement with the analysis of drag reduction with Poiseuille flows by Moarref & Jovanović (2010), who similarly found that, for boundary conditions of sufficiently long wavelength, the energy cost increased, with increasing wavelength, faster than the resulting drag reduction.

This analysis, as well as that of Hoepffner & Fukagata (2009) and Moarref & Jovanović (2010), demonstrates that, at small A (the amplitude of the boundary condition), the induced bulk flow will increase parabolically with A . (Here we are referring to the dimensional velocity \hat{u} , rather than the non-dimensionalised velocity u .) The asymptotic behaviour of the bulk flow at small $A/h\omega$ is detailed in § 7.

At higher values of A , however, the bulk flow will not increase parabolically with A . In § 4, it has been shown that, if the amplitude of the boundary condition is sufficiently greater than the speed at which it travels along the channel wall, then the effect upon the bulk flow of increasing A will diminish.

Furthermore, it been shown in § 3 that, for boundary conditions of small amplitude, there exists an optimal frequency for the boundary condition, at which the bulk flow will be maximized. Beyond this frequency, any increase will have the effect of reducing the bulk flow. In fact, the bulk flow will be reduced to zero in the limit as the frequency approaches infinity. This has been explained via an analogy with the motion of fluid adjacent to a shuffling body.

6.3. Generalizing the boundary conditions

So far, we have only considered a very narrow range of the possible boundary conditions that could be used to induce a bulk flow via transpiration. Specifically, we have considered those boundary conditions that can be expressed as single-mode travelling waves, in which boundary conditions are of equal wavelength and frequency. However, in § 3.6 we have demonstrated a method by which this perturbation analysis could be readily extended to investigate all periodic boundary conditions. This method relies upon the fact that, if a boundary condition may be expressed as a sum of two or more travelling sinusoidal waves, then the first-order approximation of the overall translational flow will be the sum of the first-order translational flows that each of those component travelling waves would induce separately as a boundary condition.

7. Conclusions

We have analysed the behaviour of fluids that are subjected to a non-zero wall-normal velocity at the surfaces of the channel. This arrangement, known also as ‘transpiration’, allows no net volume flux to be imparted upon the flow through the channel walls, and does not require the boundary conditions to remain constant over time.

We have shown, through a perturbation analysis, that the effect of convection is capable of inducing a bulk flow in a fluid that is driven by transpiration. The set of boundary conditions considered were those in which the wall-normal velocities at either wall of the channel can be expressed as travelling sine waves. The waves at either wall may differ in their magnitude, and may be out of phase, but they are of equal wavelength and frequency. The induced bulk flow is found to move in the direction counter to the motion of the boundary condition, which concurs with the results of reported numerical simulations, and perturbation analyses, of systems driven by transpiration.

The asymptotic behaviour of $\langle \hat{u} \rangle$, the average streamwise velocity (in dimensional units) within the channel, is detailed here. Again, A denotes the maximum amplitude of the boundary condition, λ its wavelength and ω its temporal frequency of oscillation, h denotes the height of the channel, and ν is the kinematic viscosity of the fluid ($\nu \equiv \mu/\rho$). The ratio of the amplitude of the boundary conditions at either

wall is denoted by γ , and the degree to which they are out of phase by ϕ . Note that, in order to obtain the bulk flow from $\langle \hat{u} \rangle$, it must be multiplied by h .

The magnitude of the average streamwise velocity in the limit as $A/h\omega \rightarrow 0$ is given in (3.6) and (3.9). In dimensional units, the average velocity is given by

$$\langle \hat{u} \rangle \sim \begin{cases} \frac{1 + \gamma^2 - 2\gamma \cos \phi}{5040} \frac{h^2 \omega A^2 \lambda}{\nu^2}, & \frac{h}{\lambda} \rightarrow 0, \frac{h^2 \omega}{\nu} \rightarrow 0, \\ \frac{1 + \gamma^2 - 2\gamma \cos \phi}{2\sqrt{2}} \frac{A^2 \lambda}{h\sqrt{\nu\omega}}, & \frac{h}{\lambda} \rightarrow 0, \frac{h^2 \omega}{\nu} \rightarrow \infty, \\ \frac{3(1 + \gamma^2)}{64} \frac{\omega A^2 \lambda^3}{\nu^2}, & \frac{h}{\lambda} \rightarrow \infty, \frac{\lambda^2 \omega}{\nu} \rightarrow 0, \\ \frac{1 + \gamma^2}{4\sqrt{2}} \frac{A^2}{\sqrt{\nu\omega}}, & \frac{h}{\lambda} \rightarrow \infty, \frac{\lambda^2 \omega}{\nu} \rightarrow \infty. \end{cases} \quad (7.1)$$

In this small- $A/h\omega$ limit, it has been found that the maximum flow is obtained by minimizing h/λ , while maintaining an optimal frequency ω_{max} , which is given by

$$\omega_{max} \approx 100 \frac{\nu}{h^2}. \quad (7.2)$$

Using the optimal frequency, as well as a wavelength that is longer than the height of the channel, we find that the average flow will be approximately

$$\langle \hat{u} \rangle \approx \frac{\lambda}{h} (1 + \gamma^2 - 2\gamma \cos \phi), \quad \lambda > h, \quad \omega = \omega_{max}. \quad (7.3)$$

Decidedly different behaviour is found when the amplitude of the boundary condition, A , is much greater than the speed at which it moves along the wall of the channel, $\lambda\omega$. In the limit as $\lambda\omega/A \rightarrow 0$, assuming that the flow remains two-dimensional, the average velocity becomes

$$\langle \hat{u} \rangle \leq O(\lambda\omega). \quad (7.4)$$

This implies that $\langle \hat{u} \rangle$ will not remain proportional to A^2 for all values of A . Moreover, as A is increased, $\partial \langle \hat{u} \rangle / \partial A$ will at some point diminish, approaching zero in the limit as $\lambda\omega/A \rightarrow 0$. It remains to be determined whether there in fact exists a bulk flow in this limit, and the direction of the flow.

This has been proved only for two-dimensional flows resulting from a limited set of the possible transpiration boundary conditions. These include the boundary conditions for which the perturbation analysis was performed. The extension of this result to three-dimensional flows and generalized boundary conditions has been posed as a conjecture.

Acknowledgements

The authors wish to acknowledge the financial support of the Australian Research Council and the University of Melbourne Postgraduate Scholarship Scheme.

Appendix A. Details of the perturbation analysis

In this section we detail the derivation mentioned in §3. This derivation is based upon the assumption that α is small, and involves expanding the velocity and pressure in α , in the manner shown in (3.1).

A.1. Perturbation methodology

Substituting (3.1) into (2.21), and equating orders of α , we obtain

$$\nabla^4 \Psi_0 - \beta \frac{\partial}{\partial t} \nabla^2 \Psi_0 = 0, \tag{A 1a}$$

$$\nabla^4 \Psi_1 - \beta \frac{\partial}{\partial t} \nabla^2 \Psi_1 = \beta \left(\frac{\partial \Psi_0}{\partial z} \frac{\partial}{\partial x} - \frac{\partial \Psi_0}{\partial x} \frac{\partial}{\partial z} \right) \nabla^2 \Psi_0, \tag{A 1b}$$

$$\begin{aligned} \nabla^4 \Psi_2 - \beta \frac{\partial}{\partial t} \nabla^2 \Psi_2 &= \beta \left(\frac{\partial \Psi_0}{\partial z} \frac{\partial}{\partial x} - \frac{\partial \Psi_0}{\partial x} \frac{\partial}{\partial z} \right) \nabla^2 \Psi_1 \\ &+ \beta \left(\frac{\partial \Psi_1}{\partial z} \frac{\partial}{\partial x} - \frac{\partial \Psi_1}{\partial x} \frac{\partial}{\partial z} \right) \nabla^2 \Psi_0, \end{aligned} \tag{A 1c}$$

...

We can see from (A 1a) that the leading-order term, Ψ_0 , represents an unsteady Stokes flow. For all except the leading-order term, our boundary conditions are that

$$\frac{\partial \Psi_n}{\partial x} = \frac{\partial \Psi_n}{\partial z} = 0 \quad \text{at } z = 0, 1 \text{ for } n > 0, \tag{A 2}$$

while the boundary conditions given within (2.13) and (2.15) apply to the leading-order term, Ψ_0 . This implies that the leading-order boundary conditions are

$$\frac{\partial \Psi_0}{\partial z} = 0, \quad \text{at } z = 0, 1, \tag{A 3}$$

$$\frac{\partial \Psi_0}{\partial x} = \begin{cases} \sin(\eta x + t), & \text{at } z = 1, \\ \gamma \sin(\eta x + t - \phi), & \text{at } z = 0. \end{cases} \tag{A 4}$$

A.2. Leading-order terms

In order to find a closed-form solution for Ψ_0 , we introduce the following assumed form, which is based upon the boundary condition at the top wall:

$$\Psi_0 = \xi_{0,1}(z) e^{i(\eta x + t)} + \xi_{0,-1}(z) e^{-i(\eta x + t)}, \tag{A 5}$$

where $\xi_{0,1}(z)$ and $\xi_{0,-1}(z)$ are functions to be determined. By substituting the above into (A 1a), then equating coefficients of $e^{i(\eta x + t)}$ and $e^{-i(\eta x + t)}$, we obtain the following differential equations:

$$\frac{d^4 \xi_{0,1}}{dz^4} - (2\eta^2 + \beta i) \frac{d^2 \xi_{0,1}}{dz^2} + \eta^2(\eta^2 + \beta i) \xi_{0,1} = 0, \tag{A 6}$$

$$\frac{d^4 \xi_{0,-1}}{dz^4} - (2\eta^2 - \beta i) \frac{d^2 \xi_{0,-1}}{dz^2} + \eta^2(\eta^2 - \beta i) \xi_{0,-1} = 0. \tag{A 7}$$

From the boundary conditions acting upon $\Psi_0(x, t)$, we can infer the boundary conditions for $\xi_{0,1}(z)$ and $\xi_{0,-1}(z)$. From (A 4), we obtain

$$\xi_{0,\pm 1} = \begin{cases} \frac{1}{2\eta}, & \text{at } z = 1, \\ \frac{\gamma}{2\eta} e^{\mp i\phi}, & \text{at } z = 0, \end{cases} \tag{A 8}$$

while from (A 3), we obtain

$$\frac{d\xi_{0,1}}{dz} = \frac{d\xi_{0,-1}}{dz} = 0 \quad \text{at } z = 0, 1. \quad (\text{A } 9)$$

From the above equations and boundary conditions, we can derive closed-form solutions,

$$\xi_{0,1} = c_1 e^{\eta z} + c_2 e^{-\eta z} + c_3 e^{Hz} + c_4 e^{-Hz}, \quad (\text{A } 10)$$

$$\xi_{0,-1} = c_1^* e^{\eta z} + c_2^* e^{-\eta z} + c_3^* e^{H^* z} + c_4^* e^{-H^* z}, \quad (\text{A } 11)$$

where

$$H \equiv \sqrt{\eta^2 + \beta i}, \quad H^* \equiv \sqrt{\eta^2 - \beta i}, \quad (\text{A } 12)$$

and the various constant coefficients c_1, c_1^*, \dots are dependent upon the choice of boundary conditions. They are given by

$$\begin{aligned} c_1 = & [8\eta(\sinh H(2\eta^2 + i\beta) \sinh \eta + 2H\eta - 2H\eta \cosh H \cosh \eta)]^{-1} \\ & \times \{e^{-H-\eta-i\phi}[\gamma(\eta(H-H) + i\beta) + e^{2H}\gamma(-\eta(H+\eta) - i\beta) + (\eta(H-H) + i\beta)] \\ & \times e^{2H+\eta+i\phi} - e^{\eta+i\phi}(\eta(H+\eta) + i\beta) + 2H\gamma\eta e^{H+\eta} + 2H\eta e^{H+i\phi}\}, \end{aligned} \quad (\text{A } 13a)$$

$$\begin{aligned} c_2 = & [8\eta(\sinh H(2\eta^2 + i\beta) \sinh \eta + 2H\eta - 2H\eta \cosh H \cosh \eta)]^{-1} \\ & \times \{e^{-H-i\phi}[-2\gamma e^{H+\eta}(H\eta \cosh H - \sinh H(\eta^2 + i\beta)) + e^{i\phi}(\eta(H-H) + i\beta)] \\ & + e^{2H+i\phi}(-\eta(H+\eta) - i\beta) + 2e^H H\gamma\eta + 2H\eta e^{H+\eta+i\phi}\}, \end{aligned} \quad (\text{A } 13b)$$

$$\begin{aligned} c_3 = & [8(2H\eta(\cosh H \cosh \eta - 1) - \sinh H(2\eta^2 + i\beta) \sinh \eta)]^{-1} \\ & \times \{e^{-H-\eta-i\phi}[-2H\gamma e^{H+\eta} + \gamma(H-\eta) + \gamma e^{2\eta}(H+\eta)] \\ & - 2H e^{\eta+i\phi} + (H-\eta) e^{H+2\eta+i\phi} + (H+\eta) e^{H+i\phi}\}, \end{aligned} \quad (\text{A } 13c)$$

$$\begin{aligned} c_4 = & [8(\sinh H(2\eta^2 + i\beta) \sinh \eta + 2H\eta - 2H\eta \cosh H \cosh(\eta))]^{-1} \\ & \times \{e^{-\eta-i\phi}[\gamma(2H e^\eta + e^{H+2\eta}(\eta-H) - e^H(H+\eta))] \\ & + e^{i\phi}(2H e^{H+\eta} - e^{2\eta}(H+\eta) - H+\eta)\}, \end{aligned} \quad (\text{A } 13d)$$

$$\begin{aligned} c_1^* = & [8\eta(-2H^*\eta(\cosh H^* \cosh \eta - 1) + \sinh H^*(2\eta^2 - i\beta) \sinh \eta)]^{-1} \\ & \times \{e^{-H^*-\eta}[(e^{2H^*} - 1)(\eta^2 - i\beta)(e^\eta - \gamma e^{i\phi}) \\ & + H^*\eta(\gamma(-e^{i\phi})(-2e^{H^*+\eta} + e^{2H^*} + 1) - e^{2H^*+\eta} + 2e^{H^*} - e^\eta)]\}, \end{aligned} \quad (\text{A } 13e)$$

$$\begin{aligned} c_2^* = & [8\eta(-2H^*\eta(\cosh H^* \cosh \eta - 1) + \sinh H^*(2\eta^2 - i\beta) \sinh \eta)]^{-1} \\ & \times \{e^{-H^*}[(e^{2H^*} - 1)(\eta^2 - i\beta)(-1 + \gamma e^{\eta+i\phi}) \\ & + H^*\eta(\gamma(-e^{i\phi})(e^{2H^*+\eta} - 2e^{H^*} + e^\eta) + 2e^{H^*+\eta} - e^{2H^*} - 1)]\}, \end{aligned} \quad (\text{A } 13f)$$

$$\begin{aligned} c_3^* = & [8(-2H^*\eta(\cosh H^* \cosh \eta - 1) + \sinh H^*(2\eta^2 - i\beta) \sinh \eta)]^{-1} \\ & \times \{e^{-H^*-\eta}[(e^{2\eta} - 1)\eta(e^{H^*} - \gamma e^{i\phi}) - H^*\eta e^{i\phi}(-2e^{H^*+\eta} + e^{2\eta} + 1) \\ & - H^*(e^{H^*+2\eta} + e^{H^*} - 2e^\eta)]\}, \end{aligned} \quad (\text{A } 13g)$$

$$\begin{aligned} c_4^* = & [8(2H^*\eta(\cosh H^* \cosh \eta - 1) + i \sinh H^*(\beta + 2i\eta^2) \sinh \eta)]^{-1} \\ & \times \{e^{-\eta}[(1 - e^{2\eta})\eta(-1 + \gamma e^{H^*+i\phi}) + H^*(\gamma e^{i\phi}(e^{H^*+2\eta} + e^{H^*} - 2e^\eta) \\ & - 2e^{H^*+\eta} + e^{2\eta} + 1)]\}. \end{aligned} \quad (\text{A } 13h)$$

We can now express $\Psi_0(\mathbf{x}, t)$ in closed form. To do so, we substitute (A 10) and (A 11) for $\xi_{0,1}$ and $\xi_{0,-1}$ into (A 5). Doing so, we arrive at

$$\begin{aligned} \Psi_0 = & (c_1 e^{\eta z} + c_2 e^{-\eta z} + c_3 e^{Hz} + c_4 e^{-Hz}) e^{i(\eta x+t)} \\ & + (c_1^* e^{\eta z} + c_2^* e^{-\eta z} + c_3^* e^{H^*z} + c_4^* e^{-H^*z}) e^{-i(\eta x+t)}. \end{aligned} \quad (\text{A } 14)$$

From this result, we can easily determine the pressure to leading order. To do so, we substitute u_0 (or $\partial\Psi_0/\partial z$) into the Stokes equation. Then, by assuming that the pressure exhibits the same streamwise scales of motion as the velocity field, we find that

$$p_0(\mathbf{x}, t) = \beta (c_2 e^{-\eta z} - c_1 e^{\eta z}) e^{i(\eta x+t)} + \beta (c_2^* e^{-\eta z} - c_1^* e^{\eta z}) e^{-i(\eta x+t)}. \quad (\text{A } 15)$$

A.3. First-order bulk flow

In order to determine the first-order correction to the streamfunction, Ψ_1 , we first substitute (3.2) into (A 1b). This produces an equation of the form

$$\nabla^4 \Psi_1 - \beta \frac{\partial}{\partial t} \nabla^2 \Psi_1 = Z_{1,0}(z) + Z_{1,2}(z) e^{2i(\eta x+t)} + Z_{1,-2}(z) e^{-2i(\eta x+t)}, \quad (\text{A } 16)$$

where $Z_{1,0}$, $Z_{1,2}$ and $Z_{1,-2}$ are known functions, which depend upon $\xi_{0,1}$ and $\xi_{0,-1}$. From this we can infer that Ψ_1 takes the form

$$\Psi_1 = \xi_{1,0}(z) + \xi_{1,2}(z) e^{2i(\eta x+t)} + \xi_{1,-2}(z) e^{-2i(\eta x+t)}, \quad (\text{A } 17)$$

where $\xi_{1,0}$, $\xi_{1,2}$ and $\xi_{1,-2}$ are functions to be determined. The functions $\xi_{1,2}(z)$ and $\xi_{1,-2}(z)$ can be determined by substituting the above into (A 16) and equating coefficients of the exponentials. This results in the following:

$$\frac{d^4 \xi_{1,\pm 2}}{dz^4} - 2(4\eta^2 \pm \beta i) \frac{d^2 \xi_{1,\pm 2}}{dz^2} + 8\eta^2(2\eta^2 \pm \beta i) \xi_{1,\pm 2} = Z_{1,\pm 2}, \quad (\text{A } 18)$$

with the boundary conditions

$$\xi_{1,\pm 2}(0) = \xi_{1,\pm 2}(1) = \frac{d\xi_{1,\pm 2}}{dz}(0) = \frac{d\xi_{1,\pm 2}}{dz}(1) = 0. \quad (\text{A } 19)$$

It is not possible to determine the translational flow term, $\xi_{1,0}(z)$, via an analogous method, since it would lead to a fourth-order differential equation with only two boundary conditions. Instead, we consider the Navier–Stokes equation expanded in Re . The first-order components of the expansion in the streamwise direction are given by

$$\beta \frac{\partial}{\partial t} u_1 + \beta \mathbf{u}_0 \cdot \nabla u_0 = -\frac{\partial}{\partial x} p_1 + \nabla^2 u_1. \quad (\text{A } 20)$$

From (A 17) we can infer that the streamwise velocity must take the form

$$u_1 = U_{1,0}(z) + U_{1,2}(z) e^{2i(\eta x+t)} + U_{1,-2}(z) e^{-2i(\eta x+t)}, \quad (\text{A } 21)$$

where $U_{1,0}$, $U_{1,2}$ and $U_{1,-2}$ are functions to be determined. By substituting the above into (A 20), and then averaging the result over the streamwise direction, we obtain

$$\frac{d^2}{dz^2} \bar{u}_1 = \frac{d^2}{dz^2} U_{1,0} = \beta \overline{\mathbf{u}_0 \cdot \nabla u_0} \equiv \beta \left(\frac{\partial \Psi_0}{\partial z} \frac{\partial}{\partial x} - \frac{\partial \Psi_0}{\partial x} \frac{\partial}{\partial z} \right) \frac{\partial \Psi_0}{\partial z}. \quad (\text{A } 22)$$

By substituting (3.2) into the above, we obtain

$$\frac{d^2}{dz^2} \bar{u}_1 = -\beta^2 \eta [c_3 c_1^* e^{(\eta+H)z} + c_4 c_1^* e^{(\eta-H)z} + c_3 c_2^* e^{(-\eta+H)z} + c_4 c_2^* e^{-(\eta+H)z}]$$

$$\begin{aligned}
& + c_1 c_3^* e^{(\eta+H^*)z} + c_1 c_4^* e^{(\eta-H^*)z} + c_2 c_3^* e^{(-\eta+H^*)z} + c_2 c_4^* e^{-(\eta+H^*)z} \\
& + 2c_3 c_3^* e^{(H+H^*)z} + 2c_3 c_4^* e^{(H-H^*)z} + 2c_4 c_3^* e^{(-H+H^*)z} \\
& + 2c_4 c_4^* e^{-(H+H^*)z}]. \tag{A 23}
\end{aligned}$$

By solving the above equation, subject to the no-slip boundary condition, we can determine \bar{u}_1 . Its value is given by

$$\begin{aligned}
\bar{u}_1 = \beta^2 \eta \left\{ \frac{c_3 c_1^*}{(\eta + H)^2} [1 - e^{(\eta+H)z} + z(e^{(\eta+H)} - 1)] + \frac{c_4 c_1^*}{(\eta - H)^2} [1 - e^{(\eta-H)z} \right. \\
+ z(e^{(\eta-H)} - 1)] + \frac{c_3 c_2^*}{(\eta - H)^2} [1 - e^{(-\eta+H)z} + z(e^{(-\eta+H)} - 1)] \\
+ \frac{c_4 c_2^*}{(\eta + H)^2} [1 - e^{-(\eta+H)z} + z(e^{-(\eta+H)} - 1)] + \frac{c_1 c_3^*}{(\eta + H^*)^2} [1 - e^{(\eta+H^*)z} \\
+ z(e^{(\eta+H^*)} - 1)] + \frac{c_1 c_4^*}{(\eta - H^*)^2} [1 - e^{(\eta-H^*)z} + z(e^{(\eta-H^*)} - 1)] \\
+ \frac{c_2 c_3^*}{(\eta - H^*)^2} [1 - e^{(-\eta+H^*)z} + z(e^{(-\eta+H^*)} - 1)] + \frac{c_2 c_4^*}{(\eta + H^*)^2} [1 - e^{-(\eta+H^*)z} \\
+ z(e^{-(\eta+H^*)} - 1)] + \frac{2c_3 c_3^*}{(H + H^*)^2} [1 - e^{(H+H^*)z} + z(e^{(H+H^*)} - 1)] \\
+ \frac{2c_3 c_4^*}{(H - H^*)^2} [1 - e^{(H-H^*)z} + z(e^{(H-H^*)} - 1)] + \frac{2c_4 c_3^*}{(H - H^*)^2} [1 - e^{(-H+H^*)z} \\
+ z(e^{(-H+H^*)} - 1)] + \left. \frac{2c_4 c_4^*}{(H + H^*)^2} [1 - e^{-(H+H^*)z} + z(e^{-(H+H^*)} - 1)] \right\}. \tag{A 24}
\end{aligned}$$

In order to determine the corresponding first-order approximation of the overall average $\langle u_1 \rangle$, we integrate \bar{u}_1 with respect to z from 0 to 1. This results in

$$\begin{aligned}
\langle u_1 \rangle = \frac{\beta^2 \eta}{2} \left\{ \frac{c_3 c_1^*}{(\eta + H)^3} [2 + \eta + H + e^{\eta+H}(\eta + H - 2)] + \frac{c_4 c_1^*}{(\eta - H)^3} [2 + \eta - H \right. \\
+ e^{\eta-H}(\eta - H - 2)] - \frac{c_3 c_2^*}{(\eta - H)^3} [2 - \eta + H + e^{-\eta+H}(-\eta + H - 2)] \\
- \frac{c_4 c_2^*}{(\eta + H)^3} [2 - \eta - H - e^{-(\eta+H)}(\eta + H + 2)] + \frac{c_1 c_3^*}{(\eta + H^*)^3} [2 + \eta + H^* \\
+ e^{\eta+H^*}(\eta + H^* - 2)] + \frac{c_1 c_4^*}{(\eta - H^*)^3} [2 + \eta - H^* + e^{\eta-H^*}(\eta - H^* - 2)] \\
- \frac{c_2 c_3^*}{(\eta - H^*)^3} [2 - \eta + H^* + e^{-\eta+H^*}(-\eta + H^* - 2)] - \frac{c_2 c_4^*}{(\eta + H^*)^3} [2 - \eta - H^* \\
- e^{-(\eta+H^*)}(\eta + H^* + 2)] + \frac{2c_3 c_3^*}{(H + H^*)^3} [2 + H + H^* + e^{H+H^*}(H + H^* - 2)] \\
+ \frac{2c_3 c_4^*}{(H - H^*)^3} [2 + H - H^* + e^{H-H^*}(H - H^* - 2)] - \frac{2c_4 c_3^*}{(H - H^*)^3} [2 - H + H^* \\
+ e^{-H+H^*}(-H + H^* - 2)] \\
- \left. \frac{2c_4 c_4^*}{(H + H^*)^3} [2 - H - H^* - e^{-(H+H^*)}(H + H^* + 2)] \right\}. \tag{A 25}
\end{aligned}$$

A.4. First-order velocity field

In order that we should be able to produce an approximation of the entire velocity field to first order, we now seek to determine $\xi_{1,2}$ and $\xi_{1,-2}$. We begin with the derivation of $\xi_{1,2}$. By substituting (3.2) into (A 1b), and equating coefficients of $e^{2i(\eta x+t)}$ in the result to that in (A 16), we find that

$$Z_{1,2} = \beta^2 \eta [c_1 c_3 (H - \eta) e^{(\eta+H)z} - c_1 c_4 (\eta + H) e^{(\eta-H)z} + c_2 c_3 (\eta + H) e^{(H-\eta)z} + c_2 c_4 (\eta - H) e^{-(\eta+H)z}]. \tag{A 26}$$

We can now determine $\xi_{1,2}$ by substituting the above into (A 18) and solving for the boundary conditions given within (A 19). This results in

$$\xi_{1,2} = k_1 e^{(\eta+H)z} + k_2 e^{(\eta-H)z} + k_3 e^{(H-\eta)z} + k_4 e^{-(\eta+H)z} + k_5 e^{2\eta z} + k_6 e^{-2\eta z} + k_7 e^{\sqrt{4\eta^2+2\beta iz}} + k_8 e^{-\sqrt{4\eta^2+2\beta iz}}, \tag{A 27}$$

where the constants k_1, k_2, \dots , depend only upon the values of β, η, γ and ϕ . Because the explicit forms of several of these constants are very cumbersome, and moreover physically unrevealing, we do not reproduce them here. We now similarly seek to derive $\xi_{1,-1}$. We again substitute (3.2) into (A 1b), this time equating the resulting coefficient of $e^{-2i(\eta x+t)}$ to that in (A 16). This gives

$$Z_{1,-2} = \beta^2 \eta [c_1^* c_3^* (\eta - H^*) e^{(\eta+H^*)z} - c_1^* c_4^* (\eta + H^*) e^{(\eta-H^*)z} + c_2^* c_3^* (\eta + H^*) e^{(H^*-\eta)z} + c_2^* c_4^* (\eta - H^*) e^{-(\eta+H^*)z}]. \tag{A 28}$$

We can now determine $\xi_{1,-2}$ via an analogous method to that used above to determine $\xi_{1,2}$. This yields

$$\xi_{1,-2} = k_1^* e^{(\eta+H^*)z} + k_2^* e^{(\eta-H^*)z} + k_3^* e^{(H^*-\eta)z} + k_4^* e^{-(\eta+H^*)z} + k_5^* e^{2\eta z} + k_6^* e^{-2\eta z} + k_7^* e^{\sqrt{4\eta^2-2\beta iz}} + k_8^* e^{-\sqrt{4\eta^2-2\beta iz}}, \tag{A 29}$$

where similarly the constants k_1^*, k_2^*, \dots , depend on the values of β, η, γ and ϕ , and are too cumbersome to be worth reproducing here.

REFERENCES

AAMO, O. M., KRSTIĆ, K. & BEWLEY, T. R. 2003 Control of mixing by boundary feedback in two-dimensional channel flow. *Automatica* **39**, 1597–1606.

BATCHELOR, B. K. 1967 *An Introduction to Fluid Dynamics*. Cambridge University Press.

BEWLEY, T. R. 2001 Flow control: new challenges for a new renaissance. *Prog. Aerosp. Sci.* **37**, 21.

BEWLEY, T. R. 2009 A fundamental limit on the balance of power in a transpiration-controlled channel flow. *J. Fluid Mech.* **632**, 443–446.

CHOI, H., MOIN, P. & KIM, J. 1994 Active turbulence control for drag reduction in wall-bounded flows. *J. Fluid Mech.* **262**, 75–110.

CORTELEZZI, L., LEE, K., KIM, J. & SPEYER, J. L. 1998 Skin-friction drag reduction via robust reduced-order linear feedback control. *Intl J. Comput. Fluid Dyn.* **11**, 79.

FUKAGATA, K., IWAMOTO, K. & KASAGI, N. 2002 Contribution of Reynolds stress distribution to the skin friction in wall-bounded flows. *Phys. Fluids* **14**, L73–L76.

FUKAGATA, K., SUGIYAMA, K. & KASAGI, N. 2009 On the lower bound of net driving power in controlled duct flows. *Physica D* **238**, 1082–1086.

VON HELMHOLTZ, H. 1868 Ueber die thatsächlichen grundlagen der geometrie. *Verh. des naturh.-med. Vereins zu Heidelberg* **5**, 1.

HOEPFFNER, J. & FUKAGATA, K. 2009 Pumping or drag reduction? *J. Fluid Mech.* **635**, 171–187.

- KARNIADAKIS, G. E. & CHOI, K.-S. 2003 Mechanisms on transverse motions in turbulent wall flows. *Annu. Rev. Fluid Mech.* **35**, 45–62.
- LADYZHENSKAYA, O. A. 1958 Global solvability of a boundary value problem for the Navier–Stokes equations in the case of two spacial dimensions. *Dokl. Akad. Nauk SSSR* **123**, 427–429.
- LADYZHENSKAYA, O. A. 1963 *The Mathematical Theory of Viscous Incompressible Flows*. Gordon and Breach.
- LEE, C., MIN, T. & KIM, J. 2008 Stability of a channel flow subject to wall blowing and suction in the form of a travelling wave. *Phys. Fluids* **20**, 101513.
- LIEU, B. K., MOARREF, R. & JOVANOVIĆ, M. 2010 Controlling the onset of turbulence by streamwise travelling waves. Part 2. Direct numerical simulation. *J. Fluid Mech.* **663**, 100–119.
- MAMORI, H., FUKAGATA, K. & HOEPFFNER, J. 2010 Phase relationship in laminar channel flow controlled by travelling-wave-like blowing or suction. *Phys. Rev. E* **81**, 046304.
- MARUSIC, I., JOSEPH, D. D. & MAHESH, K. 2007 Laminar and turbulent comparisons for channel flow and flow control. *J. Fluid Mech.* **570**, 467–477.
- MIN, T., KANG, S., SPEYER, J. L. & KIM, J. 2006 Sustained sub-laminar drag in a fully developed channel flow. *J. Fluid Mech.* **558**, 81–100.
- MOARREF, R. & JOVANOVIĆ, M. 2010 Controlling the onset of turbulence by streamwise travelling waves. Part 1. Receptivity analysis. *J. Fluid Mech.* **663**, 70–99.
- RILEY, N. 2001 Steady streaming. *Annu. Rev. Fluid Mech.* **33**, 43–65.
- STOKES, G. G. 1851 On the effect of the internal friction of fluids on the motion of pendulums. *Trans. Camb. Phil. Soc.* **9**, 8–106.
- TOMS, B. A. 1948 Some observations on the flow of linear polymer solutions through straight tubes at large Reynolds numbers. In *Proceedings of the 1st International Congress on Rheology*, 2, pp. 135–141. North Holland.
- WARHOLIC, M. D., SCHMIDT, G. M. & HANRATTY, T. J. 1999 The influence of a drag-reducing surfactant on a turbulent velocity field. *J. Fluid Mech.* **388**, 1–20.
- WHITE, C. M. & MUNGAL, M. G. 2008 Mechanics and prediction of turbulent drag reduction with polymer additives. *Annu. Rev. Fluid Mech.* **40**, 235–256.
- WHITTAKER, R. J., HEIL, M., BOYLE, J., JENSEN, O. E. & WALTERS, S. L. 2010a The energetics of flow through a rapidly oscillating tube. Part 2. Application to an elliptical tube. *J. Fluid Mech.* **648**, 123–153.
- WHITTAKER, R. J., WATERS, S. L., JENSEN, O. E., BOYLE, J. & HEIL, M. 2010b The energetics of flow through a rapidly oscillating tube. Part 1. General theory. *J. Fluid Mech.* **648**, 83–121.
- WOODCOCK, J. D., SADER, J. E. & MARUSIC, I. 2010 On the maximum drag reduction due to added polymers in Poiseuille flow. *J. Fluid Mech.* **659**, 473–483.